The Role of Mineral Colloids in the Facilitated Transport of Contaminants in Saturated Porous Media

submitted by

Menachem Elimelech

Environmental Engineering Program, Department of Chemical Engineering
Yale University, Post Office Box 208286, New Haven, Connecticut 06520-8286
203-432-2789 (phone), 203-432-7232 (fax), menachem.elimelech@yale.edu (email)

Joseph N. Ryan

Department of Civil, Environmental, and Architectural Engineering
University of Colorado, Campus Box 428, Boulder, Colorado 80309
303-492-0772 (phone); 801-327-7112 (fax); joe.ryan@colorado.edu (email)

Table of Contents

1. Colloid-Facilitated Transport of Contaminants in Laboratory and Field Experiments

1.1. Overview of Colloid-Facilitated Transport of Contaminants

In 1989, McCarthy and Zachara [1] gave credence to the growing suspicion that "mobile colloids in the subsurface environment may alter the transport of contaminants." Their review brought widespread recognition to the concept of "colloid-facilitated transport," the enhancement of contaminant transport resulting from the strong association of contaminants with mobile colloids (Figure 1). Although evidence of the role of colloids in facilitating the subsurface transport of contaminants appeared as early as 1968 [2-4], most predictions of contaminant transport were still based on two-phase equilibrium adsorption models (a dissolved phase and a sorbed, immobile phase). In some cases [5,6], these models were severely under-predicting the transport of certain strongly sorbing contaminants. McCarthy and Zachara [1] clearly emphasized the need to consider three phases in contaminant transport models (dissolved, sorbed to immobile subsurface materials, and sorbed to mobile colloids). Most importantly, their review spurred and guided a strong body of research over the last decade on colloid occurrence and properties, contaminant association with colloids, colloid transport, and colloid-based mitigation and remediation of contamination.

The goal of this review is to summarize our progress in addressing these colloid-facilitated transport issues over the last decade. The review is organized according to the three basic criteria for colloid-facilitated transport [1,7]:

1. Colloids must be present in sufficient amount to compete with the immobile subsurface materials for contaminant sorption.
2. Contaminants must associate extensively and virtually irreversibly with colloids.

3. Colloids must transport the contaminants into contaminant-free regions of the subsurface. In the remainder of this first section, we examine laboratory and field evidence of colloid-facilitated transport presented in the last decade. The second section of this review covers the types of colloids and their mechanisms of generation in subsurface environments. The third section outlines the basic mechanisms and kinetics of contaminant association with colloids. The fourth section describes the role of hydrodynamics and surface chemistry in the transport of colloids. Over the past decade, colloid-facilitated transport of contaminants has been reviewed by Buffle and van Leeuwen [8,9], Swanton [10], Ouyang et al. [11], Ryan and Elimelech [7], and Kretzschmar et al. [12].

In this review, we focus on the genesis and transport of inorganic mineral colloids and their natural organic matter coatings. Dissolved natural organic matter is also important in facilitating the transport of metals [13-16] and nonpolar organic compounds [13, 17-20], but we do not consider dissolved organic matter in this review because the genesis and transport of dissolved organic matter are governed by different mechanisms. Colloid-facilitated transport has also been attributed to bacteria [20-23] and their extracellular polymers [24], but we do not consider contaminant transport facilitated by "biocolloids" because it is unlikely that such materials would be sufficiently abundant in natural subsurface environments to significantly affect contaminant transport. We also focus on colloid generation and transport processes that occur in saturated porous media. In the unsaturated zone, the same basic criteria for colloid-facilitated transport apply, but the processes of colloid generation and transport are complicated by variable degrees of soil wetness, periodic flushing of soils by infiltrating rainfall, preferential flow path development, and other issues [25-28].

1.2. Colloid-Facilitated Transport of Contaminants in Laboratory Experiments

Over the last decade, colloid-facilitated transport experiments have been conducted in the laboratory with a wide variety of contaminants and colloids (Table 1). Colloid-facilitated transport has been demonstrated for alkaline and alkali earth cations (Cs and Sr), transition metals (Ni, Co, Cu, and Pb), oxyanions (arsenate and iodate), non-polar organic compounds (phenanthrene and pyrene) and a polar organic compound (the pesticide prochloraz). The colloids responsible for facilitated transport of these contaminants include polystyrene latex microspheres, kaolinite, goethite, hematite, and colloidal material isolated from natural soils and sediments. For the non-polar organic contaminants, colloid-facilitated transport was tested only with polystyrene latex microspheres [29,30], giving us little to assess the potential for natural colloids to facilitate the transport of such compounds. Most of these experiments present clear evidence that the presence of colloids accelerates the breakthrough of the contaminants (Figure 2).

Generally, the contaminants and colloids were selected to demonstrate that colloid-facilitated transport occurs and to assess the effect of other solution chemistry and porous media properties on colloid-facilitated transport. For example, high pH minimizes colloid deposition under most circumstances and increases the ability of colloids to facilitate contaminant transport [30,31]. High ionic strength reduced the colloid-facilitated transport of various transition metals by preventing the mobilization and transport of colloidal material from the soil porous medium [32]. In addition to its effect on colloid transport, high ionic strength also diminished the colloid-facilitated transport of cesium by kaolinite by competing for ion exchange sites on the kaolinite colloids [33]. Unfortunately, the laboratory experiments have not frequently been used to assess the extent of contaminant-colloid association needed to make colloid-facilitated transport significant. Only Sätmark et al. [31] included a non-sorbing compound (Na^+) as a control to demonstrate that strong association (such as that observed for Cs and iodate to goethite) is necessary for colloids to facilitate contaminant transport.

1.3. Colloid-Facilitated Transport of Contaminants in Field Experiments

Studies of colloid-facilitated transport in the field are dominated by actinides and transition metals (Table 2). Some of the field evidence for colloid-facilitated transport comes from assessments of actinide transport near underground deposits of uranium – so-called “natural analogue” studies [34-36]. These sites are of great interest for assessing the future performance of nuclear waste repositories. Detection of U, Th, and Ra associated with colloids in the groundwaters surrounding these deposits at distances from hundreds of meters to tens of kilometers seems to be strong evidence for colloid-facilitated transport; however, researchers must show that the colloids sampled at these distances from the deposits are not simply in equilibrium with the actinide content of the surrounding sediments. Likewise, detection of colloid-associated radionuclides near nuclear bomb test sites and nuclear waste sites [37-39] must show that the colloid-associated radionuclides are the only form to migrate over these distances. Only Magaritz et al. [40] was able to show that the metals associated with the colloid fraction recovered in their passive groundwater samplers were enriched relative to the metal content of the surrounding sediment.

In the only study to show colloid-facilitated transport of organic contaminants in the field, Villholth [41] showed that the extent of association of PAHs to colloids was linearly related to the octanol-water partition coefficient of the compounds at one field site and that colloid-facilitated transport was undetectable at another. The most significant difference between the sites was the amount of organic matter associated with the colloid phase.

The detection of colloid-associated actinides at the Cigar Lake site led Vilks et al. [36] to emphasize the need for essentially irreversible association between colloid and contaminant for colloid-facilitated transport to occur. For colloid-facilitated transport to be significant, the contaminant must remain bound to the colloid even when the colloid carries the contaminant away from the contaminant source and into regions the contaminant has not yet reached. If contaminant-colloid association were governed by equilibrium sorption, the contaminant would desorb from the colloids to re-equilibrate with the surrounding groundwater and subsurface materials. Some recent models of colloid-facilitated transport have shown very slow desorption kinetics are necessary for colloid-facilitated transport to be significant for both actinides [42] and nonpolar organic compounds [43].

Showing that colloid-facilitated transport of contaminants is occurring in the field is substantially more difficult than in the laboratory [44]. Usually, colloid-free control experiments cannot be conducted in the field to contrast contaminant transport in the absence and presence of the colloid. With this in mind, field studies must be carefully evaluated against the three criteria for colloid-facilitated transport. In addition, these three criteria should be used to design future field studies assessing colloid-facilitated transport.

The first criterion, that colloids be present, is ostensibly satisfied by all of the field studies – there certainly were colloids in the samples. To be thorough, though, we must evaluate the possibility that the colloids were mobilized during sampling and were not truly mobile in the groundwater. With the exception of Magaritz et al. [40], field studies have been conducted by pumping water samples from wells. A growing body of research indicates that sampling for colloids is representative only at low pumping rates – generally less than 1 L min^{-1} [45-49] or under passive sampling conditions [40,50]. At high pumping rates (greater than 1 L min^{-1}), shear is expected to induce the mobilization of colloids not truly mobile in the groundwater. The depth of the wells at some sites limited researchers to high-capacity pumps and high pumping rates [37,39]. The high pumping rate problem can be overcome by pumping until the colloid concentration in the groundwater has stabilized, but such a procedure was not used in these field tests. Of course, high pumping rates could mobilized colloid-associated contaminants only if the contaminants had been transported to the vicinity of the sampling well, so the presence of contaminants, whether truly mobile with colloids or not, indicates some kind of anomalous transport. Preferential flow paths, like those that might be found in the fractured tuff present at the Nevada Test Site, may also plausibly explain the rapid transport of the radionuclides.

One widely cited field study claiming colloid-facilitated transport has been disputed over proper identification of the contaminant flow path to the sampling locations. Penrose et al. [51] observed plutonium and americium associated with colloids about 3.4 km from the nearest waste source in an alluvial aquifer near Los Alamos National Laboratory. They contended that the colloids had facilitated the transport of these actinides through the alluvial aquifer. Recently, however, Marty et al. [52] used isotopic evidence to show that the plutonium could not have reached the sampling wells by subsurface transport. They contended that the plutonium was transported by surface flow and infiltrated into the aquifer at the sampling locations.

Some researchers have taken precautions to avoid assuming that colloid-facilitated transport has occurred. Notably, Gounaris et al. [53] detected metals and nonpolar organic compounds associated with colloidal phases in landfill leachate, but concluded that this association would not lead to colloid-facilitated transport. Assuming equilibrium between the aqueous, colloidal, and solid phases of the sediment, they calculated that the presence of colloids would result in decreases in retardation factors for strongly binding contaminants, but the resulting contaminant transport velocities were still negligible. It is clear from this type of calculation that the assumption of equilibrium will always indicate that colloid-facilitated transport will not be important because the contaminant will desorb from the colloids to the more abundant aquifer solids as the colloids move away from the contaminant source.

The second and third criteria, that the contaminant sorption to the colloids be strong and essentially irreversible and that the colloids and the associated contaminants were transported into contaminant-free regions of the subsurface environment, have been checked in only a piecemeal fashion. Vilks et al. [36] measured isotopic ratios of uranium and thorium to show that the actinides had been associated with colloids for as long as 8,000 y. Penrose et al. [51] measured no desorption of plutonium, but substantial desorption of americium, from colloids over 2 d equilibration periods. A more direct check of both of these criteria would involve demonstrating that the subsurface material surrounding the sampling location is relatively free of contaminants. Only Magaritz et al. [40] showed that the colloids contained greater proportions of the contaminant metals than the surrounding sediments.

1.4. When Colloid-Facilitated Transport Does Not Occur

Perhaps the most instructive assessment of colloid-facilitated transport is to examine the situations in which it did not occur (Table 3). Identifying the conditions that did not lead to colloid-facilitated transport will help delineate the transport criteria listed above. For example, how many colloids is enough to foster colloid-facilitated transport? How strong does the contaminant-colloid association have to be to allow colloid-facilitated transport to dominate? How resistant to deposition must the colloids be to observe colloid-facilitated transport?

Some of the laboratory studies described above explore changes in solution chemistry that diminish the importance of colloid-facilitated transport. Low pH and high ionic strength both inhibit colloid-facilitated transport by preventing the transport of colloids. The inclusion of sodium with cesium and iodate by Sätmark et al. [31] illustrated that colloid-facilitated transport does not occur for contaminants that do not bind strongly to colloids.

A greater number of field studies did not detect any significant colloid-facilitated transport. Kaplan et al. [38,54] investigated the transport of a set of actinides and transition metals in contaminant plume characterized by low pH (2.9-4.8). Of the actinides and metals investigated, only plutonium showed significant colloid-facilitated transport. For the others, the colloid concentration was deemed to be to low. The low pH of the contaminant plume also inhibited extensive adsorption of the actinides and metals to the colloids. Other studies also cite weak contaminant-colloid interactions as the main factor in preventing colloid-facilitated transport. Seta and Karathanasis [55] observed only a minimal contribution of colloids to the transport of atrazine through saturated soils. Atrazine is a relatively soluble polar organic compound that does not sorb strongly to colloids. Villholth [41] detected colloid-facilitated transport of a suite of polycyclic aromatic hydrocarbons (PAHs) at only one of the two creosote-contaminated sites investigated. The main difference between the sites was the amount of organic matter associated with the colloidal phase. Because the extent of PAH-colloid association was linearly related to the compounds' octanol-water partition coefficient, the organic matter fraction of the colloids was the major factor controlling the extent of PAH sorption. In a series of riverbank filtration studies covering a wide range of radionuclides and transition metals, colloid-facilitated transport was limited by colloid deposition in the riverbank sediments [56-58]. In the adjacent river water, the radionuclides and metals were extensively associated with colloids, but neither the colloids nor the metals penetrated any significant distance into the riverbank sediments.

In the following sections, we will examine the processes of colloid generation, contaminant association with colloids, and colloid transport in detail to better delineate the conditions controlling colloid-facilitated transport.

2. The Sources of Colloids in Subsurface Environments

2.1. Overview of Colloid Generation in Subsurface Environments

The first criterion for colloid-facilitated transport is that colloids must be present in sufficient amount to sorb a significant amount of the contaminant. To predict the potential for colloid-facilitated transport, we need to know the amount and nature of the colloids present in the subsurface environment. To know this, we need to know the sources of colloids – and the processes responsible for colloid generation – in the subsurface environment. McCarthy and Degueldre [59] presented a comprehensive review of colloids in the subsurface environment, concluding that colloid abundance is “promoted by geohydrochemical perturbations, including those characteristic of waste disposal sites.” Chemical perturbations can lead to precipitation of supersaturated phases as colloids or mobilization of colloids from the subsurface material. Hydrodynamic perturbations can mobilize colloids from the subsurface material by shear. Geological perturbations (i.e., tectonic activity) are thought to be responsible for colloid mobilization in fractured media [60]. In the following sections, we will focus on the genesis of colloids by (1) precipitation of supersaturated phases, (2) release of existing colloids by chemical perturbations, and (3) release of existing colloids by hydrodynamic perturbations.

2.2. Colloid Precipitation

Colloids generated by precipitation of supersaturated phases fall into two categories: (1) colloids that are hazardous because they are composed of contaminants and (2) colloids that must associate with contaminants to be hazardous. In some circles, such colloids have been dubbed “true colloids” and “pseudo-colloids,” respectively [61]. The formation of colloids from supersaturated phases is governed by both equilibrium and kinetic considerations; supersaturation is necessary for colloids to precipitate, but precipitation may be kinetically limited by nucleation conditions. We must also keep in mind that the precipitation of colloidal phases may be followed by their dissolution if supersaturation is not maintained along the colloid flow path.

Researchers investigating high-level nuclear waste disposal have frequently noted the possibility of precipitation of hydrated oxides of actinides in the “near-field environment,” the region around the waste that will be subjected to high actinide concentrations, high temperatures, and drastic geochemical gradients. Such conditions could be responsible for the reduction of a uranium(VI) solution to the less soluble uranium(IV), which would be followed by the formation of uranium(IV) oxyhydroxide colloids [62]. The likelihood of “true colloid” generation may be overestimated because accurate characterization of the colloidal phase is not always performed. For example, Saltelli et al. [63] reported that “americium colloids” leached from a vitreous waste form were effectively filtered by a glauconitic sand porous medium, but they did not determine whether the colloids were precipitated americium phases or americium adsorbed to colloidal phases generated by the glass degradation.

The precipitation of metal and metal sulfide colloid phases has been suggested as a possible means of metal accumulation in ore bodies. Laboratory studies have shown that both copper and mercury form colloidal sulfides in the 10-100 nm range [64,65]. Such small colloids would not be detected by typical groundwater sampling schemes; therefore, they might play a significant role in the bioavailability of these metals. Based on a surface water study, Benedetti and Boulègue [66] hypothesized that colloidal gold (Au(0)) may be the predominant gold species responsible for the supergene deposition of gold-bearing formations. Saunders [67] supported this concept by detecting gold textures in ore deposits that indicate colloidal transport. Gold complexes with humic substances have also been forwarded as the species contributing to supergene migration of gold [68].

The generation of so-called "pseudo-colloids," or colloids composed of non-hazardous compounds, has been reported under two different circumstances. The genesis of ferric oxyhydroxide colloids by oxidation of ferrous iron has been reported by Langmuir [69] and Liang et al. [70]. Langmuir [69] observed ferric oxyhydroxide particles in groundwater samples from coastal plain sediments in New Jersey where a geochemical gradient of increasing dissolved oxygen and decreasing ferrous iron concentrations were measured. Liang et al. [70] injected ferrous iron solutions into coastal plain sediments in South Carolina to measure the oxidation rate of ferrous iron. The product of the ferrous iron oxidation was ferric oxyhydroxide colloids. The colloidal stability of the ferric oxyhydroxide was enhanced by adsorption of natural organic matter. A geochemical gradient caused by a secondary sewage effluent plume was responsible for the formation of iron- and phosphorus-rich colloids in a Cape Cod, Massachusetts, aquifer [71]. The solubility product of vivianite ($Fe_3(PO_4)_2 \cdot 8\ H_2O$) was exceeded by a small amount in the groundwater. The size of the colloids, measured by dynamic light scattering and confirmed by scanning electron microscopy, was a relatively uniform 100 nm. It should be noted sampling at the same locations in future years did not detect ferrous phosphate colloids, emphasizing that the conditions favoring colloid precipitation may be transitory.

2.3. Release of Existing Colloids by Chemical Perturbations

Soils and sediments contain a wide distribution of particle sizes, including particles in the colloidal range, roughly 10 nm to 10 μm. These smallest particles are generally the most abundant in number [72,73]. These soil and sediment colloids are bound to larger grains by short-range chemical and physical interactions under geochemical conditions that prevailed during soil and sediment formation. When these geochemical conditions are changed, the forces binding these colloids to the grains can be reversed and colloid mobilization can be initiated. McCarthy and Degueldre [59] pointed out that waste disposal activities are the most common cause of such geochemical perturbations. Some natural processes, like salt-water intrusion, can also change the forces binding colloids to grains. In addition, microbial interactions with soil particles can affect soil stability and colloid mobilization (Chapters 3 and 7, this book).

Decreases in ionic strength cause colloid mobilization (Figure 3), an effect that has been clearly seen in laboratory columns [74-84] and field-related studies ranging from secondary oil recovery [85,86] to the sea water/freshwater interface [87-89] to artificial recharge of aquifers [90,91]. Mobilization is caused by expansion of the electrostatic double layers around like-charged colloids and grains (e.g., negatively charged clay mineral colloids and quartz grains). The extent and rate of colloid release increases as ionic strength decreases [77,80]. This effect can in theory be predicted by DLVO theory [92,93]; however, in practice, surface heterogeneities, roughness, and poor characterization of surface properties make theoretical predictions unreliable. The rate of colloid release decreases over time – weakly bound colloids are mobilized first and strongly bound colloids are mobilized last, suggesting an exponential distribution of release rate coefficient activation energies [84]. If colloids and grains are oppositely charged, decreases in ionic strength have no effect on colloid mobilization because decreases in ionic strength strengthen the electrostatic attraction between oppositely charged surfaces [94,95].

Perturbations in solution composition can also affect colloid mobilization. At the same ionic strength, monovalent ions cause more release than bivalent ions [79,82,96,97]. For example, sodium chloride will mobilize more colloids than calcium chloride (Figure 4). The calcium ion is more likely to specifically complex with mineral surface sites, resulting in less electrostatic repulsion and release. In addition, the presence of calcium chloride during colloid deposition inhibits colloid release by low ionic strength sodium chloride solutions [82]. Anion composition can affect colloid mobilization, also – Seaman and Bertsch [78] observed that calcium chloride caused the release of positively charged colloids from an iron oxyhydroxide-coated sand, while calcium sulfate did not because sulfate directly reduces the surface charge of these colloids through adsorption.

Increases in solution pH generally cause colloid mobilization [74,79,94,95,98]. The increase in pH typically increases the negative charge on the colloid and grain surfaces, thus enhancing electrostatic repulsion. In sediments cemented by iron and aluminum oxides, this effect is dramatically apparent as the pH increases above the point of zero charge of the oxide coatings. When the surface charge of the oxide cement is reversed, colloid mobilization is rapid.

The addition of anions, surfactants, and reductants to sediments often results in colloid mobilization (Figure 5) and, in some cases, permeability reduction (Figure 6). Dodecanoic acid, ascorbic acid, and natural groundwater containing about 30 mg L^{-1} organic matter all promoted colloid mobilization in a iron oxyhydroxide-coated quartz sand [94]. Ascorbic acid appeared to mobilize the predominantly kaolinite colloids by dissolving the iron oxyhydroxide cement. The dodecanoic acid and organic matter-rich groundwater caused colloid release without iron oxyhydroxide dissolution by reversing the surface charge on the iron oxyhydroxide cement. Injection of phosphate, dodecyl sulfate, oxalic acid, and ascorbic acid into an iron oxyhydroxide- and silica-coated quartz sand all caused significant colloid release [95,98]. Phosphate and dodecyl sulfate mobilized colloids by reversing the surface charge on the iron oxyhydroxide coatings. Oxalic acid and ascorbic acid both reversed surface charge and dissolved (by ligand-promoted and reductive dissolution, respectively) the iron oxyhydroxide coatings. A mixture of phosphate and ascorbic acid was most effective at mobilizing colloids in field “push-pull” experiments. Surfactants have also been known to induce substantial decreases in formation permeability when used at concentrations typical of surfactant-enhanced remediation [99-101]. Such clogging is typically caused by excessive colloid mobilization followed by deposition in pore throats. The likelihood of substantial permeability reduction (up to two orders of magnitude) increases as the colloid-sized content of the soil increases. A bioremediation effort involving the injection of a concentrated nutrient solution (phosphate, ammonium chloride, and hydrogen peroxide) also caused permeability reduction in a sand aquifer. Initially, the clogging was attributed to precipitation of iron oxides, but Weisner et al. [102] showed that the nutrient solutions caused extensive colloid mobilization that resulted in clogging.

Finally, colloids may be mobilized by the dissolution of cementing phases [94,95,98,103]. As discussed above, ascorbic acid dissolved the ferric oxyhydroxide cement in the Atlantic coastal plain sediments examined by Ryan and Gschwend [94] and Swartz and Gschwend [95,98]. Initially, Ryan and Gschwend [104,105] surmised that the same cement dissolution occurred naturally with natural organic matter acting as the electron donor for the reductive dissolution of the iron oxyhydroxides; however, laboratory experiments showed that the organic matter in the groundwater mobilized colloids by reversing surface charge of the iron oxyhydroxides rather than by dissolving them. Gschwend et al. [103] examined a fly ash disposal site in which low pH wastewater infiltrated into a calcium carbonate-cemented aquifer. The low pH groundwater dissolved the carbonate cement and released colloids.

2.4. Release of Existing Colloids by Hydrodynamic Perturbations

In the saturated subsurface environment, hydrodynamic perturbations include (1) pumping to sample groundwater and (2) flow through fractures and other preferential flow paths. In both cases, the flow velocity in the subsurface environment is elevated above normal. Under these conditions, we expected colloid mobilization to be caused primarily by shear on the attached colloids. Extensive theoretical and experimental studies of the effect of shear on colloid release have been conducted in model systems of spherical particles attached to flat walls [106-111]. From these studies, we know that the rate and extent of colloid detachment increases as the flow velocity and particle size increase. Thus, pumping and fracture flow should increase colloid mobilization, with larger particles preferentially mobilized before smaller particles.

The rate of pumping is a major concern in the collection of representative colloid-containing groundwater samples [45-49]. Puls et al. [45] showed that increases in pumping rate from 0.6 to

92 L min^{-1} increased the amount and size of colloids in samples from a metal-contaminated alluvial aquifer. Under steady-state conditions, the sample turbidity was approximately the same over the range of pumping rates. Backhus et al. [46] showed that a temporary increase in the pumping rate to 1.0 L min^{-1} from 0.1 L min^{-1} caused a large increase in sample turbidity. Kearl et al. [47] used a down-hole video camera to detect an increase in particle size occurring when the pumping rate was increased from 0.1 to 1.45 L min^{-1}. In addition to increases in colloid concentration in the samples, increases in the associated contaminants were also observed [46,48,49]. The increase in contaminant levels provides great incentive to use low flow rate pumping for regulators concerned about samples that exceed limits and action levels. In addition, those who use low flow rate pumping can take satisfaction in collecting samples that are most representative of the truly mobile contaminant and colloid load.

Colloids are relatively abundant in samples taken from free-flowing fractures in very low permeability rock [60,112,113]. Because the flow through these fractures occurs at much greater velocity than the flow through the surrounding matrix, we can consider the fracture flow to be a hydrodynamic perturbation causing colloid mobilization. In the fractures, the primary minerals weather to secondary clay minerals and oxides, and these are the minerals that appear as colloids in the fracture flow samples. Characterization of the size distributions of these colloid samples shows that the distribution is weighted slightly toward the larger sizes [60], suggesting that erosion (shear) is controlling the size distribution.

2.5. Nature and Abundance of Colloids

McCarthy and Degueldre [59] assembled an extensive review of the types and abundances of colloids found in the subsurface environment. The composition of most of the colloids is similar to the composition of the subsurface environment, indicating that most colloids are mobilized from the subsurface materials by chemical or physical perturbations. In summary, we can expect the colloidal phase to be dominated by (1) clay minerals, which are naturally present in the colloid size range, (2) amorphous silica, (3) metal oxyhydroxides, including ferric iron, aluminum, and manganese, (4) carbonates, primarily calcium, (5) colloid-sized fragments of primary minerals, mainly quartz and feldspars, and (6) associated organic matter. The abundance of these colloids ranges from 0-100 mg L^{-1}, with the higher concentrations generally correlated with the greater chemical and hydrodynamic perturbations.

Since the review by McCarthy and Degueldre [59], most of the studies examining colloid nature and abundance in subsurface environments have shown similar results. Soils from the Savannah River Site in South Carolina generated mica or vermiculite, kaolinite, Ti-rich ferric oxyhydroxide, gibbsite, and quartz [38,114]. From coastal plain sediments at the Savannah River Site, Seaman et al. [115] mobilized Al-rich goethite, kaolinite, and crandallite ($CaAl_3(PO_4)_2(OH)_2 \cdot H_2O$). These Savannah River colloids are relatively unique in having positively charged surfaces. Natural concentrations of these colloids were deemed too low to significantly contribute to colloid-facilitated transport [38]. The presence of organic matter as a coating is important for colloids of positive surface charge, like ferric and aluminum oxyhydroxides and the edges of clay minerals [25,104,114]. Atteia et al. [116] detected a mixture of mineral colloids including carbonates with coprecipitated metals in groundwater exiting a karst aquifer. The size distribution of these particles followed the Pareto power law; i.e., logarithmic decreases in colloid size corresponded to logarithmic increases in colloid number (Figure 7). Colloids recovered from fractures in granitic rocks have revealed similar size distributions [60,113]. Calcium carbonate colloids were also detected in limestone and calcic soils [117]. The transport of these colloids was implicated in the formation of calcic soil horizons.

Studies of deep crystalline rock formations being considered for nuclear waste disposal continue to produce new information about colloids in subsurface environments. In anoxic groundwater sampled from the Äpsö Hard Rock Laboratory in Sweden, Ledin et al. [112] found less than 0.1 mg L^{-1} of a ferrous iron-rich colloid phase. Upon exposure to air, submicrometer ferric oxyhydroxide and calcium carbonate colloids formed in the groundwater samples. Degueldre et al. [113] extended an initial study of the colloid content of the Grimsel Test Site in Switzerland to two other sites in deep granitic rocks and found similar results: the colloid phases were dominated by clay minerals and amorphous silica in the submicrometer size range at concentrations of less than 100 $\mu g\ L^{-1}$. When calcium and sodium concentrations in the groundwater are low, however, colloid concentrations were as high as 10 mg L^{-1}. A granitic groundwater in Spain (El Berrocal) also contained mainly clay minerals, silica, and iron, titanium, and aluminum oxyhydroxides [118]. Depending on groundwater chemistry, a variety of metal carbonates and sulfides was also detected.

3. Association of Contaminants with Colloids

3.1. Overview of Contaminant Association with Colloids

The second criterion for colloid-facilitated transport is the association of the contaminants with the colloids. We use "association" to encompass the wide range of sorption mechanisms (e.g., complexation, ion exchange, hydrophobic partitioning) that may contribute to contaminant-colloid interactions. In this section, we will show that contaminant association with colloids must be (1) extensive, or “strong,” and (2) essentially irreversible for colloid-facilitated transport to occur. Extensive contaminant-colloid association is typically characterized by a large distribution coefficient K_d. Irreversible colloid-contaminant association refers to slow desorption kinetics, where “slow” must be considered relative to the velocity of flow through the subsurface environment.

The distribution coefficient is useful for qualitatively assessing the strength of the contaminant-colloid interaction, but we must remember that its use in describing the colloid-facilitated transport process is quite limited. First, distribution coefficients are inadequate for describing contaminant association with colloids when sorption is non-linear. Second, distribution coefficients represent equilibrium sorption under specific geochemical conditions; thus, they are unsuited for representing sorption when geochemical conditions are changing along a flow path [1]. Third, we must be keenly aware of the importance of desorption kinetics when considering the potential for colloid-facilitated transport. Vilks et al. [36] asserted “if colloids are completely mobile in the subsurface, their impact on radionuclide migration will depend on colloid concentration and whether or not radionuclide attachment is reversible.” Colloid-facilitated transport will carry a contaminant from a zone in which the aqueous phase concentration of the contaminant is in equilibrium with the sorbed phase (both the mobile colloids and the immobile porous media grains) to a zone in which the contaminant is predominantly associated with the mobile colloids and not the aqueous phase. Desorption of the contaminants from the mobile colloids must be slow in this zone for colloid-facilitated transport to be important.

3.2. Contaminant-Colloid Association

In this section, we will examine the basic mechanisms of contaminant-colloid interactions for a variety of representative contaminants and colloids encountered in the subsurface environment. The contaminants examined will include cationic forms of metals (e.g., Cs^{+}, Cu^{2+}, PuO_2^{+}), anionic forms of metals (e.g., CrO_4^{2-}, AsO_4^{3-}), nonpolar organic compounds (e.g., polycyclic aromatic hydrocarbons, polychlorinated biphenyls, DDT) and polar organic compounds (e.g., atrazine). The colloids examined will include minerals with amphoteric surfaces (e.g., iron, aluminum, and manganese oxides, phyllosilicate edges, carbonates, and sulfides) and fixed charge surfaces (phyllosilicate faces), organic matter coatings on mineral phases, and bacteria. While the association of contaminants with organic matter coatings on colloids is addressed here, we do not address the association of contaminants with "dissolved" organic matter (e.g., humic and fulvic acids) even though this association leads to facilitated transport of both metals and nonpolar organic compounds in the subsurface environment. The genesis and transport of dissolved organic matter is governed by mechanisms different from those addressed in this review for colloids.

The basic mechanisms of contaminant association with colloids include surface complexation, ion exchange, and hydrophobic partitioning. Each of these sorption mechanisms has been the subject of exhaustive research summarized in recent reviews [119-124].

3.2.1. Cationic Forms of Metals

Cationic forms of metals (cations) are the most frequently reported contaminants influenced by colloid-facilitated transport (Tables 1 and 2); therefore, we should expect that their association with colloids is strong and their desorption is slow. Surface complexation and ion exchange reactions dominate cation adsorption to mineral, organic, and biological surfaces. Some cations (e.g., Cu^{2+}, Pb^{2+}) form strong surface complexes with amphoteric oxides surfaces (e.g., iron, aluminum, manganese oxides, clay mineral edges). We classify the metal-ligand complexes that form as “strong” if (1) the surface complex is formed even in the face of electrostatic repulsion between the cation and a positively charged oxide surface and (2) variations in ionic strength do not affect the extent of cation adsorption [119]. These conditions indicate the cation and surface ligand have formed a covalent bond. Adsorption of cations is limited by the number of reactive sites and the accumulation of positive charge on the oxide surface. The strength of a cation bond to a surface hydroxyl is related to the strength of the complex formed by the cation with hydroxyl ions in solution [120,125]; thus, metals like Cu^{2+} and Pb^{2+} form stronger surface complexes than Co^{2+} and Cd^{2+}. A general order of the strength of surface complex formation is, from strongest to weakest [125],

$$Fe^{3+} > Th^{4+} > UO_2^{2+} > Al^{3+} > Cr^{3+} > Cu^{2+} > Ni^{2+} > Co^{2+} > Zn^{2+} > Cd^{2+}$$

For other cations, like the alkali and alkaline earth metals, adsorption is relatively weak – electrostatic repulsion and increases in ionic strength decrease metal adsorption, indicating that covalent bonds are not formed. Cation adsorption to carbonate and sulfide surfaces is similar to their adsorption to oxide surfaces, but coprecipitation (incorporation of the cation into the carbonate or sulfide structure) must also be considered.

Cations will also adsorb to organic matter coatings on mineral surfaces. Major components of organic matter like humic and fulvic acids readily adsorb to positively charged mineral surfaces (e.g., iron and aluminum oxides and clay edges at pH values below their pH_{pzc} values). Most natural waters contain sufficient organic matter to ensure near-complete coating of such mineral surfaces. In the aqueous phase, cations are readily bound by humic and fulvic acids by formation of complexes with carboxylic, phenolic, and sulfhydryl ligands [122]. For hard metals (e.g., Fe^{3+}, Al^{3+}, UO^{2+}), complexes with carboxylic and phenolic functional groups dominate metal binding, while sulfhydryl groups strongly bind soft metals like Hg^{2+}. In some cases, the presence of organic matter increases the adsorption of cations, suggesting that the cation complexes with the organic matter [126]. In other cases, the organic matter reduces cation adsorption, suggesting that it blocks sites for cation adsorption on the mineral surface.

Cation adsorption to clay mineral faces occurs by ion exchange. Ion exchange is typically defined as the replacement of one ion by another for ions residing in the diffuse double layer arising from the mineral surface. On the faces of clay minerals, the diffuse double layer is generated by negative surface charge arising from isomorphic substitution (e.g., replacement of Si^{4+} by Al^{3+}). Clay minerals have high cation exchange capacities (10^{-5} to 10^{-3} eq g^{-1}) because adsorption sites exist between clay layers composed of tetrahedral silica and octahedral alumina sheets. The extent of cation adsorption by ion exchange increases as the cation charge increases and the cation hydrated radius decreases:

$$Rb^+ > Cs^+ > K^+ > NH_4^+ > Na^+ > Li^+$$

$$Ba^{2+} > Sr^{2+} > Ca^{2+} > Mg^{2+}$$

The adsorption of cations to ion exchange sites is dominated by attractive electrostatic interactions. These electrostatic bonds are substantially weaker than the covalent bonds that bind cations to oxide surface ligands. The alkali and alkaline earth metals are most commonly the subjects of ion exchange investigations because their adsorption is dominated by ion exchange and not surface complexation.

The kinetics of cation surface complexation depend on the strength of the cation-aquo bond; the rate-determining step in adsorption is the removal of water molecules bound to the cation. Desorption is generally much slower than adsorption [127,128], suggesting that the breaking of the cation surface complex is the rate-determining step. If the strength of the cation surface complex controls desorption kinetics as the strength of the cation-aquo complex does for adsorption, then cations at the upper end of the Irving-Williams series will desorb most slowly. The desorption kinetics of cations bound to organic matter are expected to follow the same mechanism – desorption will be slowest for the cations that adsorb most strongly. For example, Penrose et al. [51] determined that plutonium desorption from natural colloids was unmeasurable over 2 d, while americium desorption was fast, a kinetics trend that follows the hydrolysis constants for these species. Similarly, Bunzl et al. [129] measured greater loss of americium than plutonium from grassland soils exposed to radionuclide fallout. Cerling and Turner [130] showed that strontium was desorbed more rapidly than cesium from iron and manganese oxide-coated gravels in a streambed. Recent work also indicates that desorption is initially fast and then much slower owing to the initial release of more weakly bound cations [127].

Ion exchange kinetics are dominated by the relative selectivity of cations and the rate of diffusion of the cation through clay minerals. As with surface complexation, hysteresis between adsorption and desorption is often observed for ion exchange reactions, but the hysteresis cannot be attributed to the strength of ion exchange bonds. Instead, the slow desorption of cations from clay minerals is the result of diffusion of the cations into the clay mineral interlayers following their initial adsorption. Similar sorption hysteresis in soil aggregates and other minerals containing microporosity can be attributed to diffusion of the cation.

Actual measurements of desorption rates in colloid-facilitated transport experiments show some trends that support the kinetic expectations. Torok et al. [131] estimated a half-life of 6.3 h for desorption of cesium from clay mineral colloids. Smith and Comans [132] surmised that the rapid adsorption of cesium to clay-rich lake sediments was followed by slow transfer to less-exchangeable sites (half-life of 50-125 d). Following this transfer, desorption was estimated as very slow (half-life on the order of 10 y). The corresponding adsorption half-life was only 1.4 min. Tanaka and Ohnuki [133] measured half-lives of 0.17, 0.35, 0.53 min for desorption of strontium, cesium, and cobalt from natural colloids, a trend that follows the relative selectivity and strength of binding exhibited by these cations. In contrast, Saiers and Hornberger [134] modeled the colloid-facilitated transport of cesium by kaolinite and obtained a model fit that resulted in cesium desorption that was faster than the adsorption (half-lives of 0.4 and 2.8 h, respectively). Noell et al. [135] used desorption half-lives of 3.5 to 4.2 min to model the release of cesium from amorphous silica colloids, while the adsorption half-lives that best fit the breakthrough data were sometimes longer (12 min) and sometimes shorter (2.3 min).

3.2.2. Anionic Forms of Metals

Oxyanions have also been identified as contaminants for which colloid-facilitated transport has occurred (Table 1). For oxyanions and other ligands, surface complexation dominates adsorption. Adsorption to organic matter is generally prevented by electrostatic repulsion because most of the ionized functional groups in organic matter are anionic. Similarly, adsorption of oxyanions by ion exchange is negligible because positively charged minerals in nature would generally be coated by organic matter.

Most transition metal oxyanions are capable of forming strong surface complexes with amphoteric oxides surfaces. As for transition metal cations, these oxyanion surface complexes are classified as "strong" if the surface complex is formed when electrostatic repulsion prevails and variations in ionic strength do not affect the extent of adsorption. These conditions indicate the oxyanion and the surface metal have formed a covalent bond. Adsorption of oxyanions is limited by the number of reactive sites and the buildup of negative charge on the oxide surface. The strength of an oxyanion bond to a surface hydroxyl is related to the acidity of the oxyanion – weaker acids are more strongly bound to surface metal sites just as they more strongly bind protons. A general order of the strength of surface complex formation is, from strongest to weakest for adsorption to goethite [121],

$$AsO_4^{3-} > PO_4^{3-} > VO_4^{3-} > CrO_4^{2-} > SO_4^{2-} > SeO_4^{2-}$$

For anions like sulfate and selenate, adsorption is relatively weak – electrostatic repulsion and increases in ionic strength decrease their adsorption, indicating that covalent bonds are not formed.

The kinetics of metal oxyanion adsorption and desorption follows the same general trends identified for cationic forms of metals. Desorption is usually much slower than adsorption owing the formation of strong surface complexes [136]. For arsenate and chromate, adsorption on goethite occurred via a fast ligand exchange resulting in monodentate surface complexes followed by a slow ligand exchange resulting in bidentate surface complexes. Following the order of surface complex strength, chromate desorption was faster than arsenate desorption.

3.2.3. Nonpolar Organic Compounds

Nonpolar organic compounds are driven from water by unfavorable interactions with the polar solvent. If organic matter is present, it will readily absorb nonpolar organic compounds as an organic solvent would readily partition these compounds from water [123,124,137]. To a limited extent, bare mineral surfaces also accept nonpolar organic compounds driven from the water, but organic matter must be essentially absent from the system for nonpolar organic compound partitioning to mineral surfaces to occur [138]. The extent of sorption into organic matter depends on the hydrophobicity of the nonpolar organic compound, a property described by the compound's octanol-water partition coefficient K_{ow}, and the amount of organic matter. Sorption of some nonpolar organic compounds is extensive because their interactions with water are so unfavorable, but this extensive sorption is not characterized as "strong." Unlike surface complexation, only relatively weak bonds (e.g., van der Waals attraction) are formed between the nonpolar organic compound and the sorbent, organic matter. Similarities between the nonpolar organic compound and organic matter structure favor enhanced partitioning; e.g., the extent of polycyclic aromatic hydrocarbon sorption increases with increasing aromatic content of the organic matter [139].

The organic matter responsible for the sorption of nonpolar organic compounds may be dissolved in the aqueous phase or present as coatings on inorganic colloids. The dissolved phase is often isolated from water samples by ultrafiltration with typical cutoffs of >1 nm or >500 molecular weight and <10 nm or <100,000 molecular weight. Both of these phases have been shown to be important in binding nonpolar organic compounds [53,140], but the transport of the dissolved organic matter and organic matter coatings is very different. Dissolved organic matter behaves like a ligand; its transport is limited by adsorption, mainly to positively charged minerals like iron oxyhydroxides. Organic matter coatings are already adsorbed to mineral surfaces; thus, their transport follows that of the mineral colloids.

The kinetics of nonpolar organic compound sorption and desorption depend primarily on the rate of diffusion through the organic matter [124,141-145]. Significant hysteresis between sorption and desorption exists owing to diffusion of nonpolar organic compounds deeper into the organic matter after the initial absorption [146], a phenomenon that causes serious problems for pump-and-treat remediation of contaminated groundwater. In soils, desorption half-lives span the range of 0.3 to 140 d, with the shortest half-lives for smaller organic compounds (e.g., benzene, toluene, xylene) and the longest for larger organic compounds (e.g., polychlorinated biphenyls, chlorobenzenes). Desorption half-lives increase as the amount of organic matter increases, the mineral microporosity increases, and the molecular weight of the nonpolar organic compound increases. For a given contaminant, the amount of organic matter exerts the primary control on desorption rates [138,144]. Recent work indicates the presence of strongly and weakly bound contaminant fractions (or a distribution of binding site strengths) with correspondingly slower and faster desorption kinetics [142,143,145,147,148]. Extrapolating this slow desorption kinetics to colloids must be done with caution because the amount of organic matter associated with stationary soils is much greater than that associated with colloids. Because colloids will contain much less organic matter than soils and, more directly, the diffusion paths of contaminants out of the organic matter will be shorter, desorption from colloids should be significantly faster than desorption from soils.

3.2.4. Polar Organic Compounds

A variety of sorption mechanisms contribute to the sorption of polar organic compounds, especially those with ionizable functional groups, to colloidal phases. Depending on the structure of the polar organic compound, surface complexation, ion exchange, and hydrophobic partitioning may play a role in sorption [123,124]. For example, a polar organic compound like atrazine contains amino functional groups that are capable of binding metals on the surfaces of oxide minerals. The same functional groups can protonate to form a cationic compound that can be adsorbed by ion exchange to clay minerals. Finally, the K_{ow} of atrazine is $10^{2.56}$, indicating that atrazine sorption may be aided by hydrophobic partitioning to organic matter. Predicting the sorption of a polar organic compound like atrazine requires detailed knowledge of the composition of the colloidal phase.

The kinetics of polar organic compound sorption and desorption depend on which of the variety of sorption mechanisms dominate. As discussed above, the kinetics of desorption will be very slow if strong surface complexes are formed. If sorption is not strong, the desorption kinetics will be determined by the rate of the compound's diffusion from the interlayers and micropores of the minerals or organic matter.

3.3. Control of Colloid-Facilitated Transport by Contaminant-Colloid Association

Our review of colloid-facilitated transport experiments in the field and laboratory reveals an interesting dichotomy – colloid-facilitated transport is a relatively frequent occurrence for metal cations and oxyanions, but a relatively rare occurrence for organic compounds, both nonpolar and polar. Only two studies showed colloid-facilitated transport of organic compounds by natural colloids, one in the laboratory [149] and one in the field [41]. Two other studies showing colloid-facilitated transport of organic compounds used polystyrene latex microspheres, which cannot be considered representative of natural colloids. In the laboratory study by de Jonge et al. [149], only 2.5-13% of the organic compound, prochloraz, was colloid-associated, so true colloid-facilitated transport did not occur. In the field study by Villholth [41], the organic compound distribution in the sediments surrounding the down-gradient sampling wells was not measured, so we cannot be sure that true colloid-facilitated transport occurred. As noted in the introductory section, this is a shortcoming of virtually all of the colloid-facilitated transport field studies (the exception being the study by Magaritz et al. [40]).

The lack of clear evidence for significant colloid-facilitated transport of non-polar organic compounds points to the importance of desorption kinetics in determining the potential for colloid-facilitated transport (Figure 8). We know that metal cations and oxyanions can form strong covalent bonds with mineral colloids and associated organic matter, resulting in slow desorption kinetics [36]. The desorption of non-polar organic compounds from sediments is also quite slow, resulting in problems with remediation of organic compound-contaminated groundwater. Why, then, do we not many examples of colloid-facilitated transport of non-polar organic compounds in the field? Desorption of non-polar organic compounds from colloids must be relatively fast. It appears that the manner in which organic matter is associated with mineral colloids must present short path lengths for diffusion of sorbed organic compounds out of the organic matter. Note that our exclusion of the many studies showing “organic matter-facilitated transport” of organic compounds does not change this conclusion. While it is easy to facilitate the transport of organic compounds with dissolved organic matter in laboratory columns with short residence times [13,18,19], there is no field evidence that this process is important.

Recent efforts at modeling colloid-facilitated transport have emphasized the need for a kinetic approach to contaminant-colloid association [42,43,134,150,151] and that irreversible sorption or very slow desorption will greatly increase colloid-facilitated transport distances (Figure 9). Roy and Dzombak [43] emphasized that slow desorption of the contaminant from the colloid is "probably most important in enhancing transport distances of contaminants in natural systems with mobile colloids which usually occur at concentrations not exceeding a few mg L^{-1}." Finally, it is important to remember that the rate of desorption must be considered relative to the rate of water flow. In the slow-moving groundwater of a deep aquifer, only the most strongly bound contaminants will remain adsorbed to colloid long enough for colloid-facilitated transport to be considered significant. On the other hand, the transport of a wider range of contaminants could be facilitated by colloids in water infiltrating through a shallow unsaturated soil.

4. Transport of Colloids

4.1. Overview of Colloid Transport and Governing Equations

The transport of colloidal particles through granular porous media is governed by advection, dispersion, and the exchange of colloidal particles between the solid stationary matrix and bulk solution. This is commonly described by the advection-dispersion equation with appropriate terms for colloid deposition and release. For the simple case of one-dimensional transport (e.g., packed column) the governing equations are [12]:

$$\frac{\partial C}{\partial t} = D_p \frac{\partial^2 C}{\partial x^2} - \nu_p \frac{\partial C}{\partial x} - \frac{\rho_b}{\varepsilon}\frac{\partial S}{\partial t} \quad (4.1)$$

$$\frac{\rho_b}{\varepsilon}\frac{\partial S}{\partial t} = k_d C - \frac{\rho_b}{\varepsilon} k_r S \quad (4.2)$$

This set of equations describes the colloidal particle concentration in suspension *C(x,t)* and the amount of deposited colloidal particles per unit mass of the solid matrix *S(x,t)* as a function of travel distance x and time t. Here, D_p is the hydrodynamic dispersion coefficient for colloidal particles, v_p the average interstitial velocity of colloidal particles, ρ_b the solid bulk density, ε the porosity, and k_d and k_r the colloid deposition and release rate coefficients, respectively. The initial colloid deposition and release rates are generally assumed to follow first-order kinetics. Such equations have been successfully utilized by several researchers to describe colloid or bacteria transport in laboratory scale columns [152,153].

For fixed chemical and physical conditions, colloid release rate is often much smaller than the colloid deposition rate [75,154]. Furthermore, in the presence of attractive double-layer forces between colloidal particles and matrix surfaces the deposition of colloidal particles is practically irreversible [155]. In such cases, the release term in equation (4.2) can be omitted and the transport equation simplifies to

$$\frac{\partial C}{\partial t} = D_p \frac{\partial^2 C}{\partial x^2} - \nu_p \frac{\partial C}{\partial x} - k_d C \tag{4.3}$$

The above equation cannot be applied when retained particles influence the rate of colloid deposition, as often observed in colloid breakthrough experiments utilizing large amounts of colloidal particles at the column inlet [156]. In this chapter, we will focus on deposition kinetics of colloidal particles at low surface coverage, which may be appropriate to colloidal transport in subsurface environments.

In the following subsections, we will discuss the role of two important processes that are integral components of the governing equations above, namely particle advection and particle deposition/filtration. Because subsurface environments are physically and geochemically heterogeneous, the effects of such heterogeneities on particle advection and deposition will be emphasized.

4.2. Particle Advection and Role of Physical Heterogeneity

Structural heterogeneities, such as macropores and fractures, are quite common in subsurface environments. Such physical heterogeneities may create preferential flow paths for the advective fluid (i.e., water) and, thus, markedly influence the transport of colloidal particles and solutes [12,157]. Preferential flow in continuous channels and cracks occurs in soils, particularly during periods of rapid water infiltration. Lenses or layers with different texture in sandy aquifers also result in significant physical heterogeneity.

The physical heterogeneity of subsurface porous media is reflected in the spatial variation of the hydraulic conductivity, an important parameter in modeling subsurface flow. The spatial variation of hydraulic conductivity results in heterogeneous flow field that influences colloid transport and the resulting particle concentration distribution in the porous medium. For modeling purposes, two types of physical heterogeneity are commonly used: layered heterogeneity and random heterogeneity.

In a layered, physically heterogeneous subsurface porous medium, the porous medium is made up of several homogeneous layers. Thus, while each layer is homogeneous (*i.e.*, with constant hydraulic conductivity), the entire system is heterogeneous. Porous media with fractures or lenses of different texture may be described as layered heterogeneous.

In random physical heterogeneity, the hydraulic conductivity is randomly distributed in the three dimensional subsurface space. Substantial progress has been made in the past two decades to understand the random physical heterogeneity of groundwater aquifers. Evidence from field-scale hydraulic conductivity measurements indicates that the spatial distribution of hydraulic conductivity is lognormal [158,159]. It was also found that there exists a non-Gaussian behavior of the log-transformed hydraulic conductivity at relatively small scales, and that this non-Gaussian behavior shifts to Gaussian behavior as the length scale increases [160,161].

The influence of physical heterogeneity on colloidal transport is illustrated in the three examples below. These examples are taken from studies involving colloid transport in packed soil columns, a layered heterogeneous model aquifer, and a packed sand column. Figure 10 illustrates the transport of a conservative tracer and natural, in-situ mobilized soil colloids in columns packed with heterogeneous soil aggregates [154]. The soil aggregates in the column were comprised of 17% clay, 66% silt, and 17% sand (by weight); the clay mineralogy was dominated by quartz, vermiculite, illite, and kaolinite. Inspection of the breakthrough curves reveals two distinct features. First, particle breakthrough occurs much earlier than the solute tracer; that is, colloidal particles in the soil column travel considerably faster than a conservative tracer. Second, only a fraction of the injected particles is recovered at the column effluent, as indicated by the reduced peak and area of the normalized particle breakthrough compared to that of a tracer. The enhanced transport of colloidal particles compared to that of a conservative tracer is attributed to the phenomenon of size exclusion [162]. Contrary to the solute tracer, a portion of the pore space of the soil matrix is not accessible to the mobile colloidal particles. In this physical mechanism of size exclusion, the pores through which particles cannot travel are basically those smaller than the colloidal particles. The second distinct feature of the particle breakthrough curves in Figure 10 — the reduced peak and area of the normalized particle breakthrough compared to that of a solute tracer — is attributed to immobilization of colloidal particles on the surfaces of soil aggregates due to particle deposition. Particle deposition in porous media will be discussed in the next subsection.

The effect of layered-distributed physical (structural) heterogeneity on colloid transport is illustrated in Figure 11 [163]. The porous medium was divided into three horizontal layers parallel to the flow direction, with the hydraulic conductivity of the middle layer of the porous medium being twice as large as the hydraulic conductivity in the layers above and below. The colloid suspension is fed continuously (line injection) into the porous medium at the inlet boundary (x = 0), with 11 injection points set at 0.1 m intervals along the vertical z direction. Observations of the normalized concentration profiles over the entire two-dimensional porous medium domain are presented for t = 0.75 d. As shown, the fluid flows in the central layer faster than the other two layers, and most of the colloids migrate with the flow through the more permeable layer. This example points out to the paramount importance of preferential flow paths in colloid transport.

The last example is from the work of Saiers et al. [153]. In this work, silica colloid transport experiments in a structured-heterogeneous porous medium were carried out. The column was packed with concentric layers of homogeneous sand of different grain size, aligned parallel to the flow direction, thus forming a preferential flow path through the coarse grained sand. The colloid and tracer breakthrough curves are depicted in Figure 12. The first breakthrough of colloidal particles occurred after 0.2 pore volumes, due to rapid transport along the preferential flow path. A second increase in colloid concentration was observed after about 2 pore volumes, due to slower transport in the fine grained matrix. Very similar breakthrough curves were also observed for the conservative solute tracer. As shown, the experimental data were described quite well by a transport model which considers two different hydraulic conductivities.

4.3. Filtration Theory and Particle Deposition Kinetics

4.3.1. Filtration Theory for a Model Porous Medium

Filtration theories describe the deposition (capture) of colloidal particles during the initial stage of filtration (the so-called "clean-bed removal") based on fundamental concepts of mass transfer, hydrodynamics, and colloid and surface chemistry. The deposition of particles is represented by a single collector removal efficiency, usually denoted as h. The single collector efficiency is defined as the ratio of the overall particle deposition rate onto the collector to the convective transport of upstream particles toward the projected area of the collector. For an isolated spherical collector, the single collector removal efficiency is [164]

$$h = \frac{I}{UC_0 p a_c^2} \tag{4.4}$$

where C_0 is the bulk concentration, U is the fluid approach velocity, and I is the actual deposition rate on collector of radius a_c. The single collector efficiency is then related to the removal efficiency of the entire granular filter medium through a simple mass balance. For a granular filter composed of uniform spheres, the result is [164,165]

$$\ln\left(C / C_0\right) = -\frac{3}{4}\frac{(1-e)hL}{a_c} \tag{4.5}$$

Here e is the porosity and L is the depth of the granular medium in the filter. This expression can also be viewed as the logarithmic attenuation in concentration of suspended particles traveling a distance L of porous medium.

The goal of the fundamental filtration theories is to predict h for a given suspension under known physical and chemical conditions. However, current theories fail to predict h when repulsive double layer interactions predominate [164,166]. As a result, it is necessary to combine an empirical factor in predicting h. In this approach, we multiply the single collector efficiency, h_0, determined from physical considerations, by an empirical collision (attachment) efficiency, α, which describes the fraction of collisions with filter grains that results in attachment. Thus, the overall single collector removal efficiency is

$$h = a h_0 \tag{4.6}$$

where h_0 is the "favorable" single collector removal efficiency, which is calculated without the inclusion of electric double layer interaction [164,165]. The collision efficiency, α, for a given colloidal suspension, solution chemistry, and filter medium can be determined from column experiments and is usually in the range of 10^{-3} to 1 [7,164,166].

Based on numerical results obtained from the so-called "trajectory analysis" for various physical conditions (in the absence of double layer interaction), Rajagopalan and Tien [167] proposed a correlation equation for h_0. This equation accounts for the effects of hydrodynamic (viscous) interaction and van der Waals attraction on colloid deposition rate. It is given by [164,167]

$$h_0 = 4.0 A_S^{1/3} \left(\frac{D_\infty}{d_c U} \right)^{1/3} + A_S N_{LO}^{1/8} N_R^{15/8} + 3.38 \times 10^{-3} A_S N_G^{1.2} N_R^{-0.4} \tag{4.7}$$

where A_S is a porosity-dependent parameter of the Happel sphere-in-cell model, and N_{LO}, N_R, and N_G are dimensionless parameters. The term N_{LO} characterizes the van der Waals attraction and is defined as

$$N_{LO} = \frac{4A}{9pmd_p^2 U} \tag{4.8}$$

where A is being the Hamaker constant of the interacting media and d_p is the particle diameter. The parameter N_R is an aspect ratio given by

$$N_R = \frac{d_p}{d_c} \tag{4.9}$$

with d_c being the diameter of the collector. Lastly, N_G is a gravitational force number given by

$$N_G = \frac{(r_p - r) g d_p^2}{18 \ mU} \tag{4.10}$$

Here, g is the gravitational acceleration, m is the fluid viscosity, and r_p and r are the density of particles and fluid, respectively.

The single collector efficiency h is related to the so-called filter coefficient l_f through [164]

$$l_f = -\frac{3}{2}\,\frac{1-e}{d_c}\,h \tag{4.11}$$

where e is the effective porosity of the granular porous medium and d_c is the diameter of the collector grain. It can be shown that the particle deposition rate coefficient k_d used in equations (4.2) and (4.3) is related to the filter coefficient l_f and the approach velocity U by the following simple relationship [12]:

$$k_d = l_f\,U/e = -\frac{U}{e\,L}\ln\left(C/C_0\right) \tag{4.12}$$

An example illustrating the kinetics of particle deposition in a model granular porous medium is shown in Figure 13. In this figure, the deposition kinetics of two submicrometer-size latex particles in column packed with uniform glass beads is presented. Experimental collision efficiencies of these suspensions at various ionic strengths were calculated from the measured particle breakthrough curves using equations (4.5) and (4.6). Results are presented as stability curves; that is, the logarithm of the collision efficiency a as a function of the logarithm of ionic strength (KCl). As seen, the deposition rate (or collision efficiency) increases as the salt concentration is increased until the critical deposition concentration is attained. The increase in the collision efficiency with salt concentration is attributed the reduced electrostatic double layer repulsion caused by double layer compression and charge screening. Above the critical deposition concentration the deposition rate is transport limited whereas below this concentration it is controlled by the repulsive electrostatic double layer interaction.

4.3.2. Particle Deposition Kinetics in Natural Porous Media

Filtration theory can in principle be applied to describe the transport of monodisperse colloidal particles through uniform natural granular media such as packed sand columns. Filtration theory has also been applied to explain the transport behavior of colloidal particles in sandy aquifers [168]. For most natural porous media, however, such calculations can lead only to qualitative agreement because of the physical and chemical heterogeneities of natural subsurface porous media. The example below illustrates that, despite the complexity of natural porous media, the deposition kinetics behavior is indeed not much different than the deposition behavior with model systems, as the results shown earlier in Figure 13.

The deposition kinetics of soil colloids and synthetic latex particles in packed soil columns as a function of Na^+ and Ca^{2+} concentrations are depicted in Figure 14 [154]. The soil aggregates and natural colloids used are similar to those described in Figure 10. Results are presented as the logarithm of the deposition rate coefficient k_d, or the collision efficiency a, as a function of the logarithm of counter ion concentration. The results in Figure 14 demonstrate that calcium ions have a much more pronounced effect on the kinetics of particle deposition than sodium ions. Substantial particle deposition occurs at a much lower concentration of Ca^{2+} than Na^+. The critical deposition concentrations for Ca^{2+} (*ca*. 5 and 2 mM for the natural and latex particles, respectively) are much lower than those with Na^+ (*ca*. 200 mM for both the soil and latex particles). It is also rather remarkable that the colloid stability curves of the natural colloidal particles (top) are quite alike those of the synthetic carboxyl latex particles (bottom). These curves are also similar to other stability curves displayed in previously published studies with model particles and collectors (as in Figure 13) [164], despite the marked heterogeneity of the natural colloidal particles in terms of chemical composition, particle size, and morphology. The deposition behavior with Na^+ and Ca^{2+} shown above is generally in qualitative agreement with the classical Derjaguin, Landau, Verwey, and Overbeek (DLVO) theory of colloidal stability and the well-known Schulze-Hardy rule [169], whereby divalent counterions reduce colloidal stability much more effectively than monovalent counterions.

4.3.3. Role of Geochemical Heterogeneity

Solid phases in terrestrial environments exhibit both physical and chemical heterogeneity [7]. Silicates and aluminosilicates are the dominant primary minerals in the stationary solid phase, especially quartz, feldspar, micas, and clays. In addition, carbonates and the oxides of iron, aluminum, and manganese represent an important group of accessory minerals that are often present as coatings on the primary minerals and as intergranular cement. Aquifer sediments also contain a heterogeneous variety of complex organic molecules characterized by a wide range of molecular weights and compositions. These organic molecules are found attached to mineral surfaces as organic coatings or organic particulate matter occupying the interstitial regions of the stationary matrix.

Due to the presence of physical and chemical heterogeneities, most natural surfaces have an uneven, or heterogeneous charge distribution [170]. Surface charge heterogeneities can be classified in terms of scale as either macroscopic or microscopic. For deposition of colloidal particles onto heterogeneous surfaces, microscopic charge heterogeneity describes charge variations on a molecular level, whereas macroscopic charge heterogeneity refers to variations on the scale of colloidal particle dimensions or more. Microscopic charge heterogeneities arise from the regular arrangement of oppositely charged ions in the crystalline lattice, as well as from molecular-level structural defects such as kinks and screw dislocations. Macroscopic charge heterogeneity on natural surfaces results mainly from the presence of surface chemical impurities such as oxyhydroxide coatings [7,171].

Surface charge heterogeneity can be characterized by the distribution of local surface potential or charge on the mineral grains. Generally, it is not possible to assign exact values for variations in potential over the entire surface. However, a probability distribution of surface potentials may be assigned according to *a priori* knowledge or assumptions about surface characteristics. Song et al. [170] proposed two models to describe surface charge heterogeneity, namely the patchwise and random distribution models which are described below.

Patchwise heterogeneity implies that surface sites of equal potential are grouped together in macroscopic patches, each of which can be treated as a homogeneous surface. When considering large patches, it may be assumed that each patch behaves as a homogeneous, isolated surface in equilibrium with the bulk solution and that the interactions at patch boundaries can be neglected. In groundwater aquifers, macroscopic surface heterogeneities such as iron, aluminum, or manganese oxide patches on minerals are representative of large patchwise heterogeneities [7,170,172]. The simplest model of patchwise heterogeneity is the two-patch charge model, where the total surface area of the collector grains is divided into favorable and unfavorable fractions, as shown schematically in Figure 15.

Random (continuous) heterogeneity indicates that sites of equipotential are randomly distributed over the entire surface. The random distribution model may be applied to collectors whose surfaces do not have an obvious patchwise arrangement of charge distribution, such as amorphous substances. Because there is often no information available on the distribution of surface potentials, a normal distribution is generally assumed.

The patchwise and random distribution models should be regarded as mathematical representations of surface charge heterogeneity because, at the present time, there are no available methods to characterize actual charge site distribution of natural grain surfaces. Despite their limited nature, however, these models are useful means of describing the characteristics of surface charge heterogeneity as applied to particle deposition and transport.

An example for the paramount effect of patchwise geochemical heterogeneity on colloid transport in porous media is shown in Figure 16. Colloid deposition experiments with colloidal silica particles flowing through columns packed with geochemically heterogeneous sand were carried out [173]. Patchwise geochemical heterogeneity was introduced to the granular porous medium by modifying the surface chemistry of a fraction of the quartz sand grains via iron oxyhydroxide coating. The initial ("clean bed") removal efficiency increases as the degree of geochemical heterogeneity (or the fraction of iron oxyhydroxide coated sand) increases. At the initial stages of deposition, the colloid removal efficiency for the given conditions increases from little less than 2% for the clean quartz grains to 86% when 16% of the quartz grains are coated with iron oxyhydroxide. At the pH maintained during the column experiments (5.6-5.8), the iron oxyhydroxide coated sand grains are positively charged and thus provide favorable surfaces for the deposition of the negatively charged silica colloids. The results suggest that the degree of geochemical variability and the availability of favorably charged surfaces may play a major role in determining the mobility of colloids in subsurface aquatic environments. In groundwater environments having a preponderance of iron oxyhydroxides as mineral coatings and low in organic carbon, colloid mobility is likely to be severely curtailed due to the favorable conditions for attachment of colloids to surfaces.

Calculated single collector efficiencies from the breakthrough curves in Figure 16 demonstrates that the following relationship holds for patchwise heterogeneous porous media surfaces [170]:

$$h = l\,h_{\mathrm{f}} + (1 - l)h_u \tag{4.13}$$

where λ is the fraction of the grain surface which is favorable for deposition (as illustrated in Figure 15), and h_{f} and h_{u} are the single collector efficiencies for favorable (iron oxyhydroxide-coated sand) and unfavorable (clean sand) surfaces, respectively. Because $h_{\mathrm{f}} >> h_{\mathrm{u}}$ for patchwise heterogeneous surfaces, equation 4.13 simplifies to

$$h \approx l\,h_{\mathrm{f}} \tag{4.14}$$

Analysis of the breakthrough curve data in Figure 16 strongly supports this simplified expression.

5. Summary and Future Research

In this review, we have examined colloid-facilitated transport of contaminants in the subsurface environment from the perspective of three criteria required for colloid-facilitated transport to occur. First, colloids must be present in sufficient quantity to sorb the contaminants. Colloids present in groundwaters include clay minerals, iron and aluminum oxides, calcium carbonate, fragments of quartz, feldspars, and other primary minerals, and the organic matter coatings bound to the surfaces of these colloids. Concentrations of these colloids reach 100 mg L^{-1}, but typical colloid concentrations are in the 0.01 to 1 mg L^{-1} range. Most of the colloids in the subsurface environment are generated by chemical and physical perturbations that mobilize colloid-sized soil and sediment particles. Some of the chemical perturbations causing colloid mobilization include the mixing of fresh water into more saline water (artificial recharge, sea water interfaces, secondary oil recovery), changes in pH, and the introduction of contaminants that can alter the surface charge of colloids and grains or dissolve the cement binding colloids to grains. Some colloids may be generated by precipitation of supersaturated phases, but their existence may be too transitory to be of great concern in colloid-facilitated transport. Further research is needed to relate the potential for colloid mobilization to the geologic setting. The effects of preferential flow in soil macropores and fractured media on colloid mobilization also merits more detailed attention in the future.

Second, the contaminants must bind strongly and essentially irreversibly to the colloids for colloid-facilitated transport to occur. The colloids must outcompete the surrounding mineral grains for contaminants in the contaminated area, carry these contaminants ahead of the contaminant plume, and resist desorbing these contaminants when the surrounding water and mineral grains are contaminant-free. Contaminants that form surface complexes with colloids (e.g., transition metals, actinides) display the slowest desorption rates. In many cases, their adsorption can be considered irreversible with respect to the rate of groundwater flow. The rate of desorption of contaminants that sorb by weaker mechanisms (ion exchange, partition into organic matter) is limited mainly by diffusion. Their rate of desorption is still slow, but faster than that of surface-complexed contaminants. On the basis of desorption kinetics, metals and actinides are the most likely candidates for colloid-facilitated transport, a surmise confirmed by field evidence. In the future, some direct confirmation of the role of desorption kinetics in colloid-facilitated transport should be obtained, with proper consideration of the widely varying transport time scales in mind (e.g., short times during infiltration through the unsaturated zone, long times for release of actinides from a deep nuclear waste repository).

Third, the colloids carrying the contaminants must be mobile in the subsurface environment. Two factors can contribute to their mobility: minimizing collisions and avoiding attachment following collisions. Colloids of approximately 1 μm experience the fewest collisions in porous media at typical groundwater flow rates. Colloid collisions are also reduced in preferential flow paths (soil macropores, fractured media). Attachments are avoided by maintaining repulsive electrostatic interactions between colloids and grains. Generally, the chemical factors that encourage colloid generation also favor colloid transport – low ionic strength, high pH, and the presence of natural and anthropogenic species that increase surface charge or mask attachment sites. Heterogeneities in the subsurface environment lead to frequent encounters of colloids with oppositely charged mineral grains. Future research should focus on the roles of physical and chemical heterogeneity on colloid transport and better characterization of the surface properties of colloids and collector grains.

Laboratory studies suggest that colloid-facilitated transport should be a common occurrence; however, very few field studies have unequivocally demonstrated that it has occurred. To demonstrate colloid-facilitated transport in the field, future studies should focus on (1) characterizing the colloids present and developing plausible mechanisms for their generation, (2) assessing the reversibility of contaminant-colloid interaction and the presence of contaminant in the colloid, sediment, and aqueous phases beyond the contaminant plume, and (3) examining the mobility of the colloids in the subsurface environment.

LIST OF SYMBOLS

A	Hamaker's constant
A_s	porosity dependent parameter
a_c	collector radius
C	particle concentration
C_0	influent particle concentration
d_c	collector diameter
d_p	particle diameter
D_p	particle dispersion
D_∞	particle diffusion coefficient
g	gravitational acceleration constant
I	overall particle deposition rate onto a collector grain
k_d	particle deposition rate constant
k_r	particle release rate constant
L	filter bed depth
N_G	gravitational force dimensionless parameter
N_{LO}	van der Waals force dimensionless parameter
N_R	aspect ratio; $N_R=d_p/d_c$
S	amount of deposited colloidal particles per unit mass of the solid matrix
t	time
U	approach (superficial) velocity
v_p	average interstitial particle velocity
x	axial coordinate (distance)
a	collision (attachment) efficiency
e	porosity
λ_f	filter coefficient
h_0	favorable single collector removal efficiency
h_f	single collector efficiency for favorable surface fraction
h_u	single collector efficiency for unfavorable surface fraction
λ	heterogeneity parameter for favorable fraction grain surface
λ_f	filter coefficient
m	fluid viscosity
r	density of the fluid
r_b	solid bulk density
r_p	density of suspended particles

REFERENCES CITED

1. McCarthy, J. F. and Zachara, J. M. (1989). Subsurface transport of contaminants. *Environmental Science and Technology*, **23**, 496-502.
2. Champlin, J. B. F. and Eichholz, G. G. (1968). The movement of radioactive sodium and ruthenium through a simulated aquifer. *Water Resources Research*, **4**, 147-158.
3. Champlin, J. B. F. (1971). The physics of fine-particle movement through permeable aquifers. *Society of Petroleum Engineers Journal* **11**, 367-373.
4. Champlin, J. B. F. and Eichholz, G. G. (1976). Fixation and remobilization of trace contaminants in simulated subsurface aquifers. *Health Physics*, **30**, 215-219.
5. Coles, D. G. and Ramspott, L. D. (1982). Migration of ruthenium-106 in a Nevada Test Site aquifer: discrepancy between field and laboratory results. *Science*, **215**, 1235-1237.
6. Nyhan, J. W., Drennon, B. J., Abeele, W. V., Wheeler, M. L., Purtymun, W. D., Trujillo, G., Herrera, W. J., and Booth, J. W. (1985). Distribution of plutonium and americium beneath a 33-yr-old liquid waste disposal site. *Journal of Environmental Quality*, **14** , 501-509.
7. Ryan, J. N. and Elimelech, M. (1996). Colloid mobilization and transport in groundwater. *Colloids and Surfaces A: Physicochemical and Engineering Aspects*, **107**, 1-52.
8. Buffle, J. and van Leeuwen, H.P. (1992). *Environmental Particles*, Volume 1, Lewis Publishers, Chelsea, Michigan.
9. Buffle, J. and van Leeuwen, H.P. (1993). *Environmental Particles*, Volume 2, Lewis Publishers, Boca Raton, Florida.
10. Swanton, S. W. (1995). Modelling colloid transport in groundwater; The prediction of colloid stability and retention behaviour. *Advances in Colloid and Interface Science*, **54**, 129-208.
11. Ouyang, Y., Shinde, D., Mansell, R. S., and Harris, W. (1996). Colloid-enhanced transport of chemicals in subsurface environments: A review. *Critical Reviews in Environmental Science and Technology*, **26**, 189-204.
12. Kretzschmar, R., Borkovec, M., Grolimund, D., and Elimelech, M. (1999). Mobile subsurface colloids and their role in contaminant transport. *Advances in Agronomy*, **66**, 121-193.
13. Dunnivant, F., Jardine, P. M., Taylor, D., and McCarthy, J. F. (1992). Cotransport of cadmium and hexachlorobiphenyl by dissolved organic matter through columns containing aquifer material. *Environmental Science and Technology*, **26**, 360-368.
14. Marley, N. A., Gaffney, J. S., Orlandini, K. A., and Cunningham, M. M. (1993). Evidence for radionuclide transport and mobilization in a shallow, sandy aquifer. *Environmental Science and Technology*, **27**, 2456-2461.
15. Wang, E. X. and Benoit, G. (1996). Mechanisms controlling the mobility of lead in the spodosols of a northern hardwood forest ecosystem. *Environmental Science and Technology*, **30**, 2211-2219.
16. McCarthy, J. F., Sanford, W. E., and Stafford, P. L. (1998). Lanthanide field tracers demonstrate enhanced transport of transuranic radionuclides by natural organic matter. *Environmental Science and Technology*, **32**, 3901-3906.
17. Ballard, T. M. (1971). Role of humic carrier substances in DDT movement through forest soil. *Soil Science Society of America Proceedings*, **35**, 145-147.
18. Enfield, C. G. and Bengtsson, G. (1988). Macromolecular transport of hydrophobic contaminants in aqueous environments. *Ground Water*, **26**, 64-70.

19. Magee, B. R., Lion, L. W., and Lemley, A. T. (1991). Transport of dissolved organic macromolecules and their effect on the transport of phenanthrene in porous media. *Environmental Science and Technology*, **25**, 323-331.
20. Lindqvist, R. and Enfield, C. G. (1992). Biosorption of dichlorodiphenyltrichloroethane and hexachlorobenzene in groundwater and its implications for facilitated transport. *Applied and Environmental Microbiology*, **58**, 2211-2218.
21. Kim, S. and Corapcioglu, M. Y. (1996). A kinetic approach to modeling mobile bacteria-facilitated groundwater contaminant transport. *Water Resources Research*, **32**, 321-331.
22. Saiers, J. E. and Hornberger, G. M. (1996). Modeling bacteria-facilitated transport of DDT. *Water Resources Research*, **32**, 1455-1459.
23. Banaszak, J. E., Rittmann, B. E., and Reed, D. T. (1999). Subsurface interactions of actinide species and microorganisms: Implications for bioremediation of actinide-organic mixtures. *Journal of Radioanalytical and Nuclear Chemistry*, **241**, 385-435.
24. Dohse, D. M. and Lion, L. W. (1994). Effect of microbial polymers on the sorption and transport of phenanthrene in a low-carbon sand. *Environmental Science and Technology* **28**, 541-548.
25. Kaplan, D. I., Bertsch, P. M., Adriano, D. C., and Miller, W. P. (1993). Soil-borne mobile colloids as influenced by water flow and organic carbon. *Environmental Science and Technology*, **27**, 1193-1200.
26. Jacobsen, O. H., Moldrup, P., Larsen, C., Konnerup, L., and Petersen, L. W. (1997). Particle transport in macropores of undisturbed soil columns. *Journal of Hydrology*, **196**, 185-203.
27. Ryan, J. N., Illangasekare, T. H., Litaor, M. I., and Shannon, R. (1998). Particle and plutonium mobilization in macroporous soils during rainfall simulations. *Environmental Science and Technology*, **32**, 476-482.
28. Lægdsmand, M., Villholth, K.G., Ullum, M., and Jensen, K.H. (1999). Processes of colloid mobilization and transport in macroporous soil monoliths. *Geoderma*, **93**, 33-59.
29. Sojitra, I., Valsaraj, K. T., Reible, D. D., and Thibodeaux, L. J. (1995). Transport of hydrophobic organics by colloids through porous media 1. Experimental results. *Colloids and Surfaces A: Physicochemical and Engineering Aspects*, **94**, 197-211.
30. Roy, S. B. and Dzombak, D. A. (1997). Chemical factors influencing colloid-facilitated transport of contaminants in porous media. *Environmental Science and Technology*, **31**, 656-664.
31. Sätmark, B., Albinsson, Y., and Liang, L. (1996). Chemical effects of goethite colloids on the transport of radionuclides through a quartz-packed column. *Journal of Contaminant Hydrology*, **21**, 231-241.
32. Amrhein, C., Mosher, P. A., and Strong, J. E. (1993). Colloid-assisted transport of trace metals in roadside soils receiving deicing salts. *Soil Science Society of America Journal*, **57**, 1212-1217.
33. Saiers, J. E. and Hornberger, G. M. (1999). The influence of ionic strength on the facilitated transport of cesium by kaolinite colloids. *Water Resources Research*, **35**, 1713-1727.
34. Airey, P. L. (1986). Radionuclide migration around uranium ore bodies in the Alligator Rivers region of the Northern Territory of Australia -- Analogue of radioactive waste repositories -- A review. *Chemical Geology*, **55**, 255-268.
35. Short, S. A., Lowson, R. T., and Ellis, J. (1988). ^{234}U/238U and ^{230}Th/^{234}U activity ratios in the colloidal phases of aquifers in lateritic weathered zones. *Geochimica et Cosmochimica Acta*, **52**, 2555-2563.

36. Vilks, P., Cramer, J. J., Bachinski, D. B., Doern, D. C., and Miller, H. G. (1993). Studies of colloids and suspended particles, Cigar Lake uranium deposit, Saskatchewan, Canada. *Applied Geochemistry*, **8**, 605-616.
37. Buddemeier, R. W. and Hunt, J. R. (1988). Transport of colloidal contaminants in groundwater: Radionuclide migration at the Nevada Test Site. *Applied Geochemistry*, **3**, 535-548.
38. Kaplan, D. I., Hunter, D. B., Bertsch, P. M., Bajt, S., and Adriano, D. C. (1994). Application of synchrotron x-ray fluorescence spectroscopy and energy dispersive x-ray analysis to identify contaminant metals on groundwater colloids. *Environmental Science and Technology*, **28**, 1186-1189.
39. Kersting, A. B., Efurd, D. W., Finnegan, D. L., Rokop, D. J., Smith, D. K., and Thompson, J. L. (1999). Migration of plutonium in ground water at the Nevada Test Site. *Nature*, **397**, 56-59.
40. Magaritz, M., Amiel, A. J., Ronen, D., and Wells, M. C. (1990). Distribution of metals in a polluted aquifer: A comparison of aquifer suspended material to fine sediments of the adjacent environment. *Journal of Contaminant Hydrology*, **5**, 333-347.
41. Villholth, K. G. (1999). Colloid characterization and colloidal phase partitioning of polycyclic aromatic hydrocarbons in two creosote-contaminated aquifers in Denmark. *Environmental Science and Technology*, **33**, 691-699.
42. Smith, P. A. and Degueldre, C. (1993). Colloid-facilitated transport of radionuclides through fractures. *Journal of Contaminant Hydrology*, **13**, 143-166.
43. Roy, S. B. and Dzombak, D. A. (1998). Sorption nonequilibrium effects on colloid-enhanced transport of hydrophobic organic compounds in porous media. *Journal of Contaminant Hydrology*, **30**, 179-200.
44. Honeyman, B. D. (1999). Geochemistry -- Colloidal culprits in contamination. *Nature*, **397**, 23-24.
45. Puls, R. W., Clark, D.A., Bledsoe, B., Powell, R. M., and Paul, C. J. (1992). Metals in ground water: sampling artifacts and reproducibility. *Hazardous Waste & Hazardous Materials*, **9**, 149-162.
46. Backhus, D. A., Ryan, J. N., Groher, D. M., MacFarlane, J. K., and Gschwend, P. M. (1993). Sampling colloids and colloid-associated contaminants in ground water. *Ground Water*, **31**, 466-479.
47. Kearl, P. M., Korte, N. E., Stites, M., and Baker, J. (1994). Field comparison of micropurging vs. traditional ground water sampling. *Ground Water Monitoring and Remediation*, 183-190.
48. Bangsund, W. J. and Kangas, K. W. (1998). Representative groundwater sampling using low-flow methods. *TAPPI Journal*, **81(12)**, 129-136.
49. Creasey, C. L. and Flegal, A. R. (1999). Elemental analyses of groundwater: demonstrated advantage of low-flow sampling and trace-metal clean techniques over standard techniques. *Hydrogeology Journal*, **7**, 161-167.
50. Weisbrod, N., Ronen, D., and Nativ, R. (1996). New method for sampling groundwater colloids under natural gradient flow conditions. *Environmental Science and Technology*, **30**, 3094-3100.
51. Penrose, W. R., Polzer, W. L., Essington, E. H., Nelson, D. M., and Orlandini, K. A. (1990). Mobility of plutonium and americium through a shallow aquifer in a semiarid region. *Environmental Science and Technology*, **24**, 228-234.

52. Marty, R. C., Bennett, D., and Thullen, P. (1997). Mechanism of plutonium transport in a shallow aquifer in Mortandad Canyon, Los Alamos National Laboratory, New Mexico. *Environmental Science and Technology*, **31**, 2020-2027.
53. Gounaris, V., Anderson, P. R., and Holsen, T. M. (1993). Characteristics and environmental significance of colloids in landfill leachate. *Environmental Science and Technology*, **27**, 1381-1387.
54. Kaplan, D. I., Bertsch, P. M., and Adriano, D. C. (1995). Facilitated transport of contaminant metals through an acidified aquifer. *Ground Water*, **33**, 708-717.
55. Seta, A. K. and Karathanasis, A. D. (1997). Atrazine adsorption by soil colloids and co-transport through subsurface environments. *Soil Science Society of America Journal*, **61**, 612-617.
56. von Gunten, H. R., Waber, U. E., and Krähenbühl, U. (1988). The reactor accident at Chernobyl: A possibility to test colloid-controlled transport of radionuclides in a shallow aquifer. *Journal of Contaminant Hydrology*, **2**, 237-247.
57. Waber, U. E., Lienert, C., and von Gunten, H. R. (1990). Colloid-related infiltration of trace metals from a river to shallow groundwater. *Journal of Contaminant Hydrology*, **6**, 251-265.
58. Lienert, C., Short, S. A., and von Gunten, H. R. (1994). Uranium infiltration from a river to shallow groundwater. *Geochimica et Cosmochimica Acta*, **58**, 5455-5463.
59. McCarthy, J. F. and Degueldre, C. (1993). Sampling and characterization of colloids and particles in groundwater for studying their role in contaminant transport. In *Environmental Particles*, Volume 2, ed. Buffle, J. and van Leeuwen, H.P. Lewis Publishers, Boca Raton, Florida, 247-315.
60. Degueldre, C., Baeyens, B., Goerlich, W., Riga, J., Verbist, J., and Stadelmann, P. (1989). Colloids in water from a subsurface fracture in granitic rock, Grimsel Test Site, Switzerland. *Geochimica et Cosmochimica Acta*, **53**, 603-610.
61. Kim, J. I. (1991). Actinide colloid generation in groundwater. *Radiochimica Acta*, **52/53**, 71-81.
62. Ho, C. H. and Miller, N. H. (1985). Effect of humic acid on uranium uptake by hematite particles. *Journal of Colloid and Interface Science*, **106**, 281-288.
63. Saltelli, A., Avogadro, A., and Bidoglio, G. (1984). Americium filtration in glauconitic sand columns. *Nuclear Technology*, **67**, 245-254.
64. Horzempa, L. M. and Helz, G. R. (1979). Controls on the stability of sulfide sols: colloidal covellite as an example. *Geochimica et Cosmochimica Acta*, **43**, 1645-1650.
65. Ravichandran, M., Aiken, G. R., Ryan, J. N., and Reddy, M. M. (1999). Inhibition of precipitation and aggregation of metacinnabar (mercuric sulfide) by dissolved organic matter isolated from the Florida Everglades. *Environmental Science and Technology*, **33**, 1418-1423.
66. Benedetti, M. F. and Boulègue, J. (1991). Mechanism of gold transfer and deposition in a supergene environment. *Geochimica et Cosmochimica Acta*, **55**, 1539-1547.
67. Saunders, J. A. (1998). Silica and gold textures in bonanza ores of the Sleeper Deposit, Humboldt County, Nevada: Evidence for colloids and implications for epithermal ore-forming processes. *Economic Geology*, **89**, 628-638.
68. Bowell, R. J., Gize, A. P., and Foster, R. P. (1993). The role of fulvic acid in the supergene migration of gold in tropical rain forest soils. *Geochimica et Cosmochimica Acta*, **57**, 4179-4190.

69. Langmuir, D. (1969). Geochemistry of iron in a coastal-plain ground water of the Camden, New Jersey, area. *U.S. Geological Survey Professional Paper*, **650-C**, C224-C235.
70. Liang, L., McCarthy, J. F., Jolley, L. W., McNabb, J. A., and Mehlhorn, T. L. (1993). Iron dynamics: Transformation of Fe(II)/Fe(III) during injection of natural organic matter in a sandy aquifer. *Geochimica et Cosmochimica Acta*, **57**, 1987-1999.
71. Gschwend, P. M. and Reynolds, M. D. (1987). Monodisperse ferrous phosphate colloids in an anoxic groundwater plume. *Journal of Contaminant Hydrology*, **1**, 309-327.
72. Borkovec, M., Wu, Q., Degovics, G., Laggner, P., and Sticher, H. (1993). Surface area and size distributions of soil particles. *Colloids and Surfaces A: Physicochemical and Engineering Aspects*, **73**, 65-76.
73. Grout, H., Wiesner, M. R., and Bottero, J. Y. (1999). Analysis of colloidal phases in urban stormwater runoff. *Environmental Science and Technology*, **33**, 831-839.
74. Kallay, N., Barouch, E., and Matijevic, E. (1987). Diffusional detachment of colloidal particles from solid/solution interfaces. *Advances in Colloid and Interface Science*, **27**, 1-42.
75. McDowell-Boyer, L. M. (1992). Chemical mobilization of micron-sized particles in saturated porous media under steady flow conditions. *Environmental Science and Technology*, **26**, 586-593.
76. Nocito-Gobel, J. and Tobiason, J. E. (1996). Effects of ionic strength on colloid deposition and release. *Colloids and Surfaces A: Physicochemical and Engineering Aspects*, **107**, 223-231.
77. Ryan, J. N. and Gschwend, P. M. (1994). Effects of ionic strength and flow rate on colloid release: Relating kinetics to intersurface potential energy. *Journal of Colloid and Interface Science*, **164**, 21-34.
78. Seaman, J. C., Bertsch, P. M., and Miller, W. P. (1995). Chemical controls on colloid generation and transport in a sandy aquifer. *Environmental Science and Technology*, **29**, 1808-1815.
79. Kaplan, D. I., Sumner, M. E., Bertsch, P. M., and Adriano, D. C. (1996). Chemical conditions conducive to the release of mobile colloids from ultisol profiles. *Soil Science Society of America Journal*, **60**, 269-274.
80. Fauré, M.-H., Sardin, M., and Vitorge, P. (1996). Transport of clay particles and radioelements in a salinity gradient: Experiments and simulations. *Journal of Contaminant Hydrology*, **21**, 255-267.
81. Fauré, M.-H., Sardin, M., and Vitorge, P. (1997). Release of clay particles from an unconsolidated clay-sand core: Experiments and modelling. *Journal of Contaminant Hydrology*, **26**, 169-178.
82. Roy, S. B. and Dzombak, D. A. (1996). Colloid release and transport processes in natural and model porous media. *Colloids and Surfaces A: Physicochemical and Engineering Aspects*, **107**, 245-262.
83. Roy, S. B. and Dzombak, D. A. (1998). Na^{+}--Ca^{2+} exchange effects in the detachment of latex colloids deposited in glass bead porous media. *Colloids and Surfaces A: Physicochemical and Engineering Aspects*, **119**, 133-139.
84. Grolimund, D. and Borkovec, M. (1999). Long-term release kinetics of colloidal particles from natural porous media *Environmental Science and Technology*, **33**, 4054-4060.
85. Khilar, K. C. and Fogler, H. S. (1984). The existence of a critical salt concentration for particle release. *Journal of Colloid and Interface Science*, **101**, 214-224.

86. Sarkar, A. K. and Sharma, M. M. (1990). Fines migration in two-phase flow. *Journal of Petroleum Technology*, 646-652.
87. Goldenberg, L. C., Magaritz, M., and Mandel, S. (1983). Experimental investigation on irreversible changes of hydraulic conductivity on the seawater-freshwater interface in coastal aquifers. *Water Resources Research*, **19**, 77-85.
88. Goldenberg, L. C., Magaritz, M., Amiel, A. J., and Mandel, S. (1984). Changes in hydraulic conductivity of laboratory sand-clay mixtures caused by a seawater-freshwater interface. *Journal of Hydrology*, **70**, 329-336.
89. Goldenberg, L. C. (1985). Decrease of hydraulic conductivity in sand at the interface between seawater and dilute clay suspensions. *Journal of Hydrology*, **78**, 183-199.
90. Nightingale, H. I. and Bianchi, W. C. (1977). Ground-water turbidity resulting from artificial recharge. *Ground Water*, **15**, 146-152.
91. Brown, D. L. and Silvey, W. D. (1977). Artificial recharge to a freshwater-sensitive brackish-water sand aquifer, Norfolk, Virginia. *U.S. Geological Survey Professional Paper*, **939**.
92. Derjaguin, B. V. and Landau, L. (1941). Theory of the stability of strongly charged lyophobic sols and the adhesion of strongly charged particles in solutions of electrolytes. *Acta Physicochimica URSS*, **14**, 633-662.
93. Verwey, E. J. W. and Overbeek, J. Th. G. (1948). *Theory of the Stability of Lyophobic Colloids*, Elsevier, Amsterdam.
94. Ryan, J. N. and Gschwend, P. M. (1994). Effects of solution chemistry on clay colloid mobilization from an iron oxide-coated sand aquifer. *Environmental Science and Technology*, **28**, 1717-1726.
95. Swartz, C. H. and Gschwend, P. M. (1998). Mechanisms controlling release of colloids to groundwater in a Southeastern Coastal Plain aquifer sand. *Environmental Science and Technology*, **32**, 1779-1785.
96. Frenkel, H., Goertzen, J. O., and Rhoades, J. D. (1978). Effects of clay type and content, exchangeable sodium percentage, and electrolyte concentration on clay dispersion and soil hydraulic conductivity. *Soil Science Society of America Journal*, **42**, 32-39.
97. Shainberg, I., Rhoades, J. D., and Prather, R. J. (1980). Effect of low electrolyte concentration on clay dispersion and hydraulic conductivity of a sodic soil. *Soil Science Society of America Journal*, **45**, 273-277.
98. Swartz, C. H. and Gschwend, P. M. (1999). Field studies of in situ colloid mobilization in a Southeastern Coastal Plain aquifer. *Water Resources Research*, **35**, 2213-2223.
99. Allred, B. and Brown, G. O. (1994). Surfactant-induced reductions in soil hydraulic conductivity. *Ground Water Monitoring and Remediation*, 174-184.
100. Allred, B. and Brown, G. O. (1995). Surfactant-induced reductions of saturated hydraulic conductivity and unsaturated diffusivity. *American Chemical Society Symposium Series*, **594**, 216-230.
101. Renshaw, C. E., Zynda, G. D., and Fountain, J. C. (1997). Permeability reductions induced by sorption of surfactant. *Water Resources Research*, **33**, 371-378.
102. Wiesner, M. R., Grant, M. C., and Hutchins, S. R. (1996). Reduced permeability in groundwater remediation systems: Role of mobilized colloids and injected chemicals. *Environmental Science and Technology*, **30**, 3184-3191.
103. Gschwend, P. M., Backhus, D. A., MacFarlane, J. K., and Page, A. L. (1990). Mobilization of colloids in groundwater due to infiltration of water at a coal ash disposal site. *Journal of Contaminant Hydrology*, **6**, 307-320.

104. Ryan, J. N. and Gschwend, P. M. (1990). Colloid mobilization in two Atlantic Coastal Plain aquifers: Field studies. *Water Resources Research*, **26**, 307-322.
105. Ryan, J. N. and Gschwend, P. M. (1992). Effect of iron diagenesis on the transport of colloidal clay in an unconfined sand aquifer. *Geochimica et Cosmochimica Acta*, **56**, 1507-1521.
106. O'Neill, M. E. (1968). A sphere in contact with a plane wall in a slow linear shear flow. *Chemical Engineering Science*, **23**, 1293-1298.
107. Hubbe, M. A. (1984). Theory of detachment of colloidal particles from flat surfaces exposed to flow. *Colloids and Surfaces*, **12**, 151-178.
108. Sharma, M. M., Chamoun, H., Sita Rama Sarma, D. S. H., and Schechter, R. S. (1992). Factors controlling the hydrodynamic detachment of particles from surfaces. *Journal of Colloid and Interface Science*, **149**, 121-134.
109. Amirtharajah, A. and Raveendran, P. (1993). Detachment of colloids from sediments and sand grains. *Colloids and Surfaces A: Physicochemical and Engineering Aspects*, **73**, 211-227.
110. Das, S. K., Schechter, R. S., and Sharma, M. M. (1994). The role of surface roughness and contact deformation on the hydrodynamic detachment of particles from surfaces *Journal of Colloid and Interface Science*, **164**, 63-77.
111. Govindaraju, R. S., Reddi, L. N., and Kasavaraju, S. K. (1995). A physically based model for mobilization of kaolinite particles under hydraulic gradients. *Journal of Hydrology*, **172**, 331-350.
112. Ledin, A., Karlsson, S., Düker, A., and Allard, B. (1994). Measurements in situ of concentration and size distribution of colloidal matter in deep groundwaters by photon correlation spectroscopy. *Water Research*, **28**, 1539-1545.
113. Degueldre, C., Pfeiffer, H.-R., Alexander, W., Wernli, B., and Bruetsch, R. (1996). Colloid properties in granitic groundwater systems. I: Sampling and characterisation. *Applied Geochemistry*, **11**, 677-695.
114. Kaplan, D.I., Bertsch, P.M., and Adriano, D.C. (1997). Mineralogical and physicochemical differences between mobile and nonmobile colloidal phases in reconstructed pedons. *Soil Science Society of America Journal*, **61**, 641-649.
115. Seaman, J. C., Bertsch, P. M., and Strom, R. N. (1997). Characterization of colloids mobilized from southeastern coastal plain sediments. *Environmental Science and Technology*, **31**, 2782-2790.
116. Atteia, O., Perret, D., Adatte, T., Kozel, R., and Rossi, P. (1998). Characterization of natural colloids from a river and spring in a karstic basin. *Environmental Geology*, **34**, 257-269.
117. Baghernejad, M. and Dalrymple, J. B. (1993). Colloidal suspensions of calcium-carbonate in soils and their likely significance in the formation of calcic horizons. *Geoderma*, **58**, 17-41.
118. Turrero, M.-J., Gómez, P., Pérez del Villar, L., Moulin, V., Magonthier, M.-C., and Menager, M.-T. (1995). Relation between colloid composition and the environment of their formation: application to the El Berrocal site (Spain). *Applied Geochemistry*, **10** , 119-131.
119. Davis, J. A. and Kent, D. B. (1990). Surface complexation modeling in aqueous geochemistry. In *Mineral-Water Interface Geochemistry*, ed. Hochella, M.F.Jr. and White, A.F. Mineralogical Society of America, *Reviews in Mineralogy*, **23**, 177-260.
120. Dzombak, D. A. and Morel, F. M. M. (1990). *Surface Complexation Modeling: Hydrous Ferric Oxide*, John Wiley & Sons, New York.
121. Stumm, W. (1992). *Chemistry of the Solid-Water Interface*, Wiley-Interscience, New York.

122. Senesi, N. (1992). Metal-humic substance complexes in the environment. Molecular and mechanistic aspects by multiple spectroscopic approach. In *Biogeochemistry of Trace Metals*, ed. Adriano, D.C. Lewis Publishers, Boca Raton, Florida, 429-496.
123. Senesi, N. (1993). Nature of interactions between organic chemicals and dissolved humic substances and the influence of environmental factors. In *Organic Substances in Soil and Water: Natural Constituents and Their Influences on Contaminant Behavior*, ed. Beck, A.J., Jones, K.C., Hayes, M.H.B., and Mingelgrin, U. Royal Society of Chemistry, Cambridge, 73-101.
124. Schwarzenbach, R. P., Gschwend, P. M., and Imboden, D. M. (1993). *Environmental Organic Chemistry*, John Wiley & Sons, New York.
125. Dugger, D. L., Stanton, J. H., Irby, B. N., McConnell, B. L., Cummings, W. W., and Maatman, R. W. (1964). The exchange of twenty metal ions with the weakly acidic silanol group of silica gel. *Journal of Physical Chemistry*, **68**, 757-760.
126. Ledin, A., Karlsson, S., Düker, A., and Allard, B. (1994). The adsorption of europium to colloidal iron oxyhydroxides and quartz -- the impact of pH and an aquatic fulvic acid. *Radiochimica Acta*, **66/67**, 213-220.
127. Strawn, D. G., Scheidegger, A., and Sparks, D. L. (1998). Kinetics and mechanisms of Pb(II) sorption and desorption at the aluminum oxide-water interface. *Environmental Science and Technology*, **32**, 2596-2601.
128. Lu, N., Cotter, C. R., Kitten, H. D., Bentley, J., and Triay, I. R. (1998). Reversibility of sorption of plutonium-239 onto hematite and goethite colloids. *Radiochimica Acta*, **83**, 167-173.
129. Bunzl, K., Flessa, H., Kracke, W., and Schimmack, W. (1995). Association of fallout $^{239+240}$Pu and ^{241}Am with various soil components in successive layers of a grassland soil. *Environmental Science and Technology* **29**, 2513-2518.
130. Cerling, T. E. and Turner, R. R. (1982). Formation of freshwater Fe-Mn coatings on gravel and the behavior of ^{60}Co, ^{90}Sr, and ^{137}Cs in a small watershed. *Geochimica et Cosmochimica Acta*, **46**, 1333-1343.
131. Torok, J., Buckley, L. P., and Woods, B. L. (1990). The separation of radionuclide migration by solution and particle transport in soil. *Journal of Contaminant Hydrology*, **6**, 185-203.
132. Smith, J. T. and Comans, R. N. J. (1996). Modelling the diffusive transport and remobilisation of ^{137}Cs in sediments: The effects of sorption kinetics and reversibility. *Geochimica et Cosmochimica Acta*, **60**, 995-1004.
133. Tanaka, T. and Ohnuki, T. (1996). Colloidal migration behavior of radionuclides sorbed on mobile fine soil particles through a sand layer. *Journal of Nuclear Science and Technology*, **33**, 62-68.
134. Saiers, J. E. and Hornberger, G. M. (1996). The role of colloidal kaolinite in the transport of cesium through laboratory sand columns. *Water Resources Research*, **32**, 33-41.
135. Noell, A. L., Thompson, J. L., Corapcioglu, M. Y., and Triay, I. R. (1998). The role of silica colloids on facilitated cesium transport through glass bead columns and modeling. *Journal of Contaminant Hydrology*, **31**, 23-56.
136. Grossl, P. R., Eick, M. J., Sparks, D. L., Goldberg, S., and Ainsworth, C. C. (1997). Arsenate and chromate retention mechanisms on goethite. 2. Kinetic evaluation using a pressure-jump relaxation technique. *Environmental Science and Technology*, **31**, 321-326.
137. Karickhoff, S. W. (1981). Semi-empirical estimation of sorption of hydrophobic pollutants on natural sediments and soils. *Chemosphere*, **10**, 833-846.

138. Piatt, J. J., Backhus, D. A., Capel, P. D., and Eisenreich, S. J. (1996). Temperature-dependent sorption of naphthalene, phenanthrene, and pyrene to low organic carbon aquifer sediments. *Environmental Science and Technology*, **30**, 751-760.
139. Chin, Y.-P., Aiken, G. R., and Danielsen, K. M. (1997). Binding of pyrene to aquatic and commercial humic substances: The role of molecular weight and aromaticity. *Environmental Science and Technology*, **31**, 1630-1635.
140. Backhus, D. A. and Gschwend, P. M. (1990). Fluorescent polycyclic aromatic hydrocarbons as probes of studying the impact of colloid on pollutant transport in groundwater. *Environmental Science and Technology*, **24**, 1214-1223.
141. Mackay, A. A., Chin, Y.-P., MacFarlane, J. K., and Gschwend, P. M. (1996). Laboratory assessment of BTEX soil flushing. *Environmental Science and Technology*, **30**, 3223-3231.
142. Werth, C. J. and Reinhard, M. (1997). Effects of temperature on trichloroethylene desorption from silica gel and natural sediments. 2. Kinetics. *Environmental Science and Technology*, **31**, 697-703.
143. Cornelissen, G., van Noort, P. C. M., Parsons, J. R., and Govers, H. A. J. (1997). Temperature dependence of slow adsorption and desorption kinetics of organic compounds in sediments. *Environmental Science and Technology*, **31**, 454-460.
144. Cornelissen, G., van Noort, P. C. M., and Govers, H. A. J. (1998). Mechanism of slow desorption of organic compounds from sediments: A study using model sorbents. *Environmental Science and Technology*, **32**, 3124-3131.
145. Schlebaum, W., Schraa, G., and van Riemsdijk, W. (1999). Influence of nonlinear sorption kinetics on the slow-desorbing organic contaminant fraction in soil. *Environmental Science and Technology*, **33**, 1413-1417.
146. Aochi, Y. O. and Farmer, W. J. (1997). Role of microstructural properties in the time-dependent sorption/desorption behavior of 1,2-dichloroethane on humic substances. *Environmental Science and Technology*, **31**, 2520-2526.
147. Culver, T. B., Hallissey, S. P., Sahoo, D., Deitsch, J. J., and Smith, J. A. (1997). Modeling the desorption of organic contaminants from long-term contaminated soil using distributed mass transfer rates. *Environmental Science and Technology*, **31**, 1581-1588.
148. Ten Hulscher, Th. E. M., Vrind, B. A., van den Heuvel, H., van der Velde, L. E., Beurskens, J. E. M., and Govers, H. A. J. (1999). Triphasic desorption of highly resistant chlorobenzenes, polychlorinated biphenyls, and polycyclic aromatic hydrocarbons in field contaminated soil. *Environmental Science and Technology*, **33**, 126-132.
149. de Jonge, H., Jacobsen, O. H., de Jonge, L. W., and Moldrup, P. (1998). Particle-facilitated transport of prochloraz in undisturbed sandy loam soil columns. *Soil Science Society of America Journal*, **27**, 1495-1503.
150. van de Weerd, H. and Leijne, A. (1997). Assessment of the effect of kinetics on colloid facilitated transport in porous media. *Journal of Contaminant Hydrology*, **26**, 245-256.
151. van de Weerd, H., Leijne, A., and van Riemsdijk, W. (1998). Transport of reactive colloids and contaminants in groundwater: Effect of nonlinear kinetic interactions. *Journal of Contaminant Hydrology*, **32**, 313-331.
152. McCaulou, D. R., Bales, R. C., and McCarthy, J. F. (1994). Use of short-pulse experiments to study bacteria transport through porous media. *Journal of Contaminant Hydrology*, **15** , 1-14.
153. Saiers, J. E., Hornberger, G. M., and Harvey, C. (1994). Colloidal silica transport through structured, heterogeneous porous media. *Journal of Hydrology*, **163**, 271-288.

154. Grolimund, D., Elimelech, M., Borkovec, M., Barmettler, K., Kretzschmar, R., and Sticher, H. (1998). Transport of in situ mobilized colloidal particles in packed soil columns. *Environmental Science and Technology*, **32**, 3562-3569.
155. Elimelech, M. (1991). Kinetics of capture of colloidal particles in packed beds under attractive double layer interactions. *Journal of Colloid and Interface Science*, **146**, 337-351.
156. Song, L. and Elimelech, M. (1993). Dynamics of colloid deposition in porous media: Modeling the role of retained particles. *Colloids and Surfaces A: Physicochemical and Engineering Aspects*, **73**, 49-63.
157. Toran, L. and Palumbo, A. V. (1992). Colloid transport through fractured and unfractured laboratory sand columns. *Journal of Contaminant Hydrology*, **9**, 289-303.
158. Freeze, R.A. (1975). A stochastic-conceptual analysis of one-dimensional groundwater flow in nonuniform homogeneous media. *Water Resources Research*, **11**, 725-741.
159. Sudicky, E.A. (1986) A natural gradient experiment on solute transport in a sand aquifer: Spatial variability of hydraulic conductivity and its role in the dispersion process. *Water Resources Research*, **22**, 2069-2082.
160. Painter, S. (1996). Evidence for non-Gaussian scaling behavior in heterogeneous sedimentary formations. *Water Resources Research*, **32**, 1183-1195.
161. Liu, H.H. and Molz, F.J. (1997). Comment on “Evidence for non-Gaussian scaling behavior in heterogeneous sedimentary F. J. formations” by Scott Painter. *Water Resources Research*, **33**, 907-908.
162. Kessler, J. H. and Hunt, J. R. (1994). Dissolved and colloidal contaminant transport in a partially clogged fracture. *Water Resources Research*, **30**, 1195-1206.
163. Sun, N., Elimelech, M., Sun, N.-Z., and Ryan, J.N. (in press). A two-dimensional model of colloid transport in physically and geochemically heterogeneous porous media. *Journal of Contaminant Hydrology*.
164. Elimelech, M., Gregory, J., Jia, X., and Williams, R. (1995). *Particle Deposition & Aggregation. Measurement, Modelling and Simulation*, Butterworth-Heinemann, Oxford, England.
165. Yao, K.-M., Habibian, M. T., and O'Melia, C. R. (1971). Water and wastewater treatment filtration: Concepts and applications. *Environmental Science and Technology*, **5**, 1105-1112.
166. Elimelech, M. and O'Melia, C. R. (1990). Kinetics of deposition of colloidal particles in porous media. *Environmental Science and Technology*, **24**, 1528-1536.
167. Rajagopalan, R. and Tien, C. (1976). Trajectory analysis of deep-bed filtration with the sphere-in-cell porous media model. *American Institute of Chemical Engineering Journal*, **22**, 523-533.
168. Harvey, R. W. and Garabedian, S. P. (1991). Use of colloid filtration theory in modeling movement of bacteria through a contaminated sandy aquifer. *Environmental Science and Technology*, **25**, 178-185.
169. Hiemenz, P. C. (1986). *Principles of Colloid and Surface Chemistry*, Marcel Dekker, New York.
170. Song, L., Johnson, P. R., and Elimelech, M. (1994). Kinetics of colloid deposition onto heterogeneously charged surfaces in porous media. *Environmental Science and Technology*, **28**, 1164-1171.
171. Coston, J. A., Fuller, C. C., and Davis, J. A. (1995). Pb^{2+} and Zn^{2+} adsorption by a natural aluminum- and iron-bearing surface coating on aquifer sand. *Geochimica et Cosmochimica Acta*, **59**, 3535-3547.

172. Ryan, J. N., Elimelech, M., Ard, R. A., Harvey, R. W., and Johnson, P. R. (1999). Bacteriophage PRD1 and silica colloid transport and recovery in an iron oxide-coated sand aquifer. *Environmental Science and Technology*, **33**, 63-73.
173. Johnson, P. R., Sun, N., and Elimelech, M. (1996). Colloid transport in geochemically heterogeneous porous media: Modeling and measurements. *Environmental Science and Technology*, **30**, 3284-3293.
174. Puls, R. W. and Powell, R. M. (1992). Transport of inorganic colloids through natural aquifer material: Implications for contaminant transport. *Environmental Science and Technology*, **26**, 614-621.
175. Grolimund, D., Borkovec, M., Barmettler, K., and Sticher, H. (1996). Colloid-facilitated transport of strongly sorbing contaminants in a natural porous media: A laboratory column study. *Environmental Science and Technology*, **30**, 3118-3123.
176. Seta, A. K. and Karathanasis, A. D. (1997). Stability and transportability of water-dispersible soil colloids. *Soil Science Society of America Journal*, **61**, 604-611.

Table 1. A compilation of recent colloid-facilitated subsurface transport of contaminants in laboratory experiments. Travel times noted as either time or number of pore volumes (PV).

contaminant	colloids	porous media	travel time and distance	comments	reference
Co, Sr, Cs	clay minerals from porous media; neutron-activated for colloid tracing	course sand (90%) and clay or zeolite (10%)	56 h 15 cm	high sodium phosphate concentration from waste form	Torok et al. [131]
arsenate	hematite 100-300 nm 5-10 mg L^{-1}	alluvial sand and gravel; quartz, feldspar	up to 4 PV 0.8-3.4 m d^{-1} 2.5-5.1 cm	I 0.03 mol L^{-1}	Puls and Powell [174]
Cu, Pb, Ni, Cr	clay and organic matter	calcareous loam soil	~10 cm	0.1 mol L^{-1} NaCl 0.1 mol L^{-1} CaMg-acetate	Amrhein et al. [32]
phenanthrene, pyrene	polystyrene latex 76, 301 nm	glass 0.1, 0.2 mm quartz sand ~0.12 mm	250 PV 20 cm	0, 0.0005 mol L^{-1} KCl	Sojitra et al. [29]
Pb	clay minerals from soil; ~0.5-1 μm diameter	silt loam soil; non-calcareous	0.3 to 1 h 10-12 cm	0.02-0.050 mol L^{-1} NaCl 0.00015 mol L^{-1} $CaCl_2$	Grolimund et al. [175]
Cs	montmorillonite	quartz sand	30 PV	0.05-0.5 mol L^{-1} NaCl	Fauré et al. [80]
Cs	kaolinite 0-200 mg L^{-1} ~0.5 μm	quartz sand	100 PV 5.2 cm	I 0.002-0.1 mol L^{-1} pH 7.2	Saiers and Hornberger [33,134]
Cs, iodate	goethite 6-28 mg L^{-1} 0.12 μm	quartz sand	7.5-60 min 6.0 cm	I 0.001 mol L^{-1} pH 4.0, 10.5	Sätmark et al. [31]
Cs, Sr, Co	natural colloids from soil <5 μm	sandy soil; quartz, feldspar	1-10 cm	pH 6.7	Tanaka and Ohnuki [133]
Ni	natural colloids from Lincoln sand 250 mg L^{-1}	Ottawa sand	10 cm	I 0.001 mol L^{-1} pH 8.3	Roy and Dzombak [30]
phenanthrene	latex microspheres 100 mg L^{-1}	Eustis sand	10 cm	I 0.001 mol L^{-1} pH 7.5, 9.8	Roy and Dzombak [30]
Cs	silica 100 nm 200 mg L^{-1}	glass beads 150-210 μm, 355-420 μm	10 PV 50 cm	pH 8.9 $NaHCO_3$/ Na_2CO_3	Noell et al. [135]
prochloraz (*N*-propyl-*N*-[2-(2,4,6-trichlorophenoxy)ethyl] imidazole-1-carboxamide)	uncharacterized; mobilized from soil	undisturbed sandy loam soil	27 h 20 cm	2.5-13% in colloidal phase	de Jonge et al. [149]

Table 2. A compilation of recent colloid-facilitated subsurface transport of contaminants in field experiments.

contaminant	colloids	porous media	travel time and distance	comments	reference
U, Th	quartz, muscovite, lepidocrocite, 1:1 and 2:1 clay minerals; 10k MWCO	Alligator River U deposit, Australia; carbonate minerals, tuff; variable saturation	<1 to 14 km	0.01-2.0% ^{238}U and 0.3-39% ^{230}Th in colloid phase	Airey [34]; Short et al. [35]
Mn, Co, Ce, Eu, Ru, Sb, Cs	quartz, feldspar, clay minerals	Nevada Test Site; fractured rhyolitic lava and tuff	~25 y 300 m		Buddemeier and Hunt [37]
Zn, Cu, Ag	30-60 mg L^{-1}	carbonate-rich sand, clay layers	20 y 30 m vertical transport	secondary sewage effluent irrigation	Magaritz et al. [40]
U, Th, Ra	illite, chlorite, kaolinite, iron oxyhydroxide, quartz, organic matter; 100-400 nm; 1-8 mg L^{-1}	Cigar Lake U deposit, Saskatchewan, Canada; fractured and geochemically altered sandstone	up to ~300 m	large (>10^3 mL g^{-1})and variable K_d values indicate “irreversible” sorption	Vilks et al. [36]
Pu, Th	kaolinite, goethite, gibbsite; positively charged	sand, silt, clay; positively charged	6-11 d 1.02 km	pH 2.9-4.8; Pu and Th transported by colloids	Kaplan et al. [38]
PAHs	clay minerals, iron oxyhydroxide, iron sulfide, quartz >10 nm, ~5 mg L^{-1}, 18% organic matter	marine sands; creosote contamination	80 m	5-35% in colloid phase; linear K_{oc}-K_{ow} relationship	Villholth [41]
Cs, Co, Eu, Pu	illite, smectite, zeolites 7 nm to >1 μm	Nevada Test Site; fractured rhyolitic lava and tuff	1-80 m y^{-1} 1.3 km	>90% in colloid phases	Kersting et al. [39]

Table 3. A compilation of recent laboratory and field experiments showing that colloid-facilitated transport did not significantly contribute to the subsurface transport of the contaminant. Travel times noted as either times or number of pore volumes (PV).

contaminant	colloids	porous media	travel time and distance	comments	reference
Ru, I, Te, Cs	clay minerals, 2-450 nm	River Glatt banks; glaciofluvial sand and gravel; quartz, feldspar, carbonates, illite, chlorite	2 d 5 m	<2.5% in colloid phase; colloid filtration in riverbank	von Gunten et al. [56]
Cu, Cd, Zn	clay minerals, 2-450 nm	River Glatt banks (see above)	2 d 5 m	<2% in colloid phase; colloid filtration in riverbank	Waber et al. [57]
U	clay minerals, 2-450 nm	River Glatt banks (see above)	2 d 5 m	only 4% in colloid phase; colloid filtration in riverbank	Lienert et al. [58]
Pu, Am	uncharacterized; >0.45 µm	Mortandad Canyon, Los Alamos National Laboratory; alluvial sand, silt, clay	~30 y 3.3 km	flow path disputed; isotopic evidence indicates surface flow	Penrose et al. [51]; Marty et al. [52]
Am, Cs, Cr, Ni, Cu, Cd, Pb, U	kaolinite, goethite, gibbsite; positively charged	sand, silt, clay; positively charged	6-11 d 1.02 km	pH 2.9-4.8; colloid concentrations too low; metals not adsorbed	Kaplan et al. [38,54]
Na	goethite 6-28 mg L^{-1} 0.12 µm	quartz sand	7.5-60 min 6.0 cm	weak Na-goethite association	Sätmark et al. [31]
atrazine (2-chloro-4-ethylamino-6-isopropylamino-*s*-triazine	clay minerals mobilized from six soils	six undisturbed soils	6 PV 20 cm	2-18% transport enhancement not caused directly by association with colloids	Seta and Karathanasis [55,176]
PAHs	clay minerals, iron oxyhydroxide, iron sulfide, quartz >10 nm ~5 mg L^{-1} 10% organic matter	glacial sands; creosote contamination	200 m	lower organic matter fraction	Villholth [41]

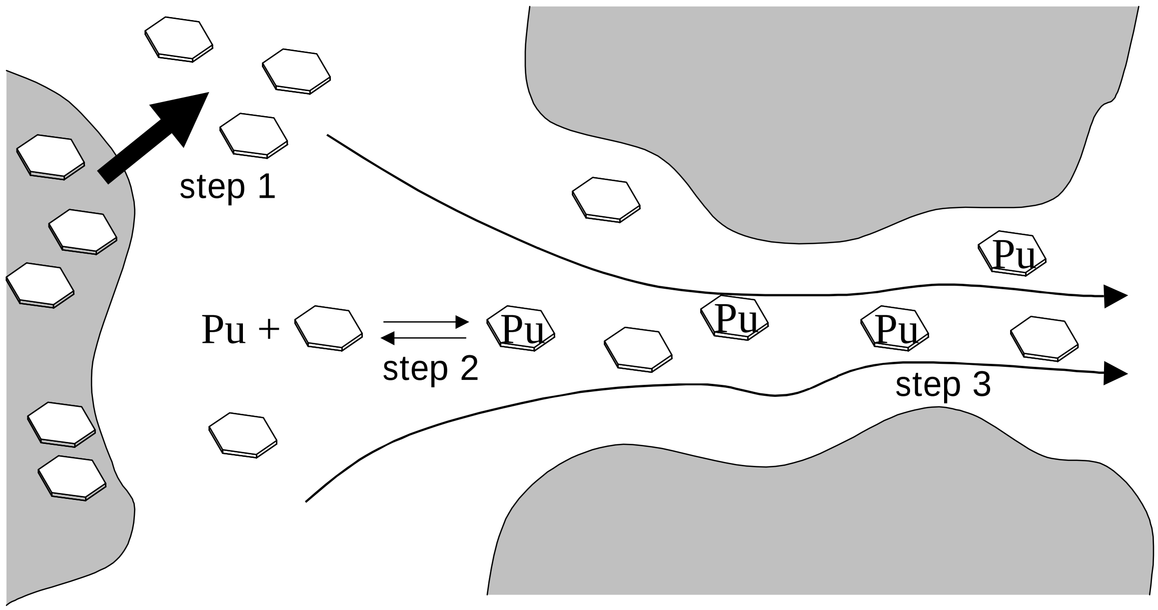

Figure 1. A schematic summary of the processes controlling colloid-facilitated transport: (1) colloid generation, (2) contaminant association with colloids, and (3) colloid transport.

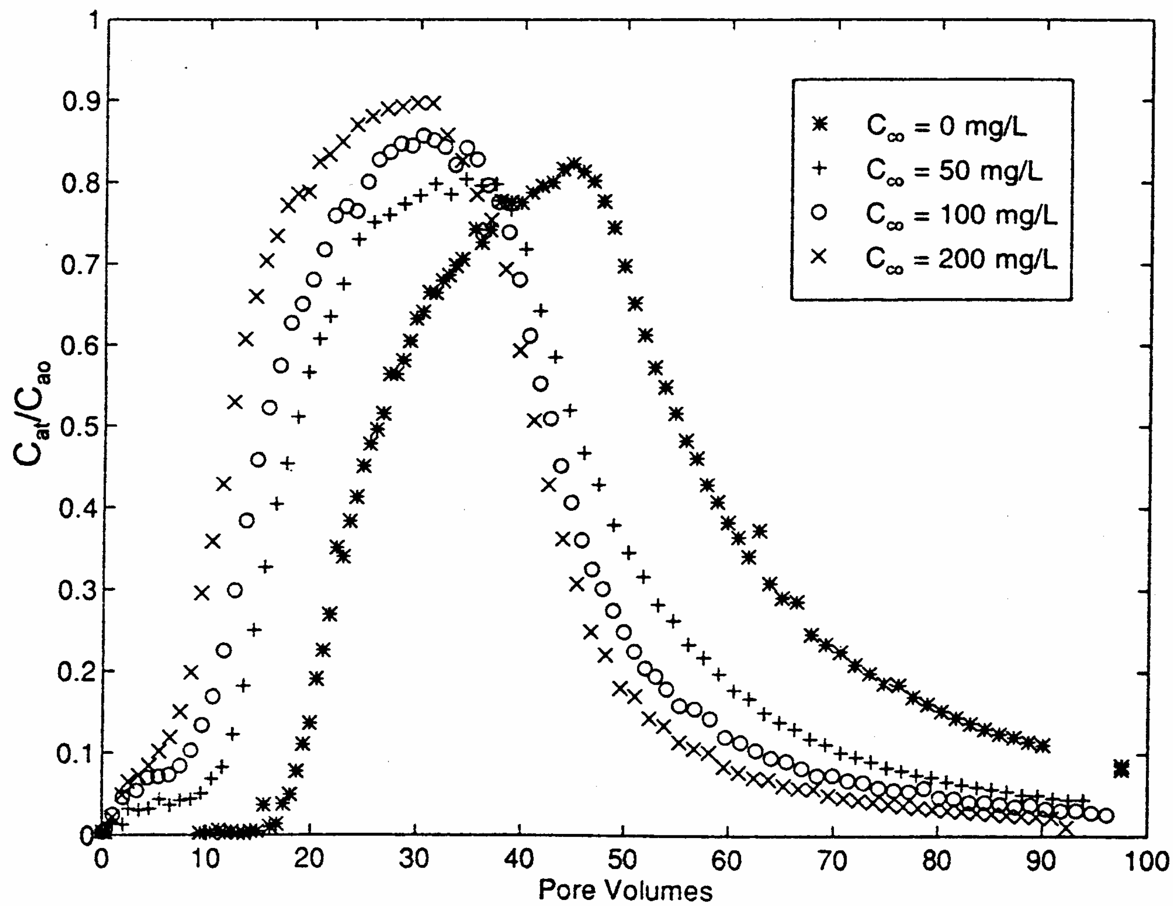

Figure 2. The presence of kaolinite colloids facilitates the transport of cesium in a quartz sand column [134]. The normalized breakthrough of cesium-137 (a ratio of C_{at}, the total mobile ^{137}Cs concentration in the column effluent, and C_{ao}, the total concentration of ^{137}Cs in the column influent) through a quartz sand column as a function of the concentration of kaolinite colloids (C_8). The number of pore volumes required for breakthrough decreases as the colloid concentration increases because a greater fraction of the cesium-137 is adsorbed to the colloids. The kaolinite colloids achieve breakthrough in the quartz sand column in one pore volume.

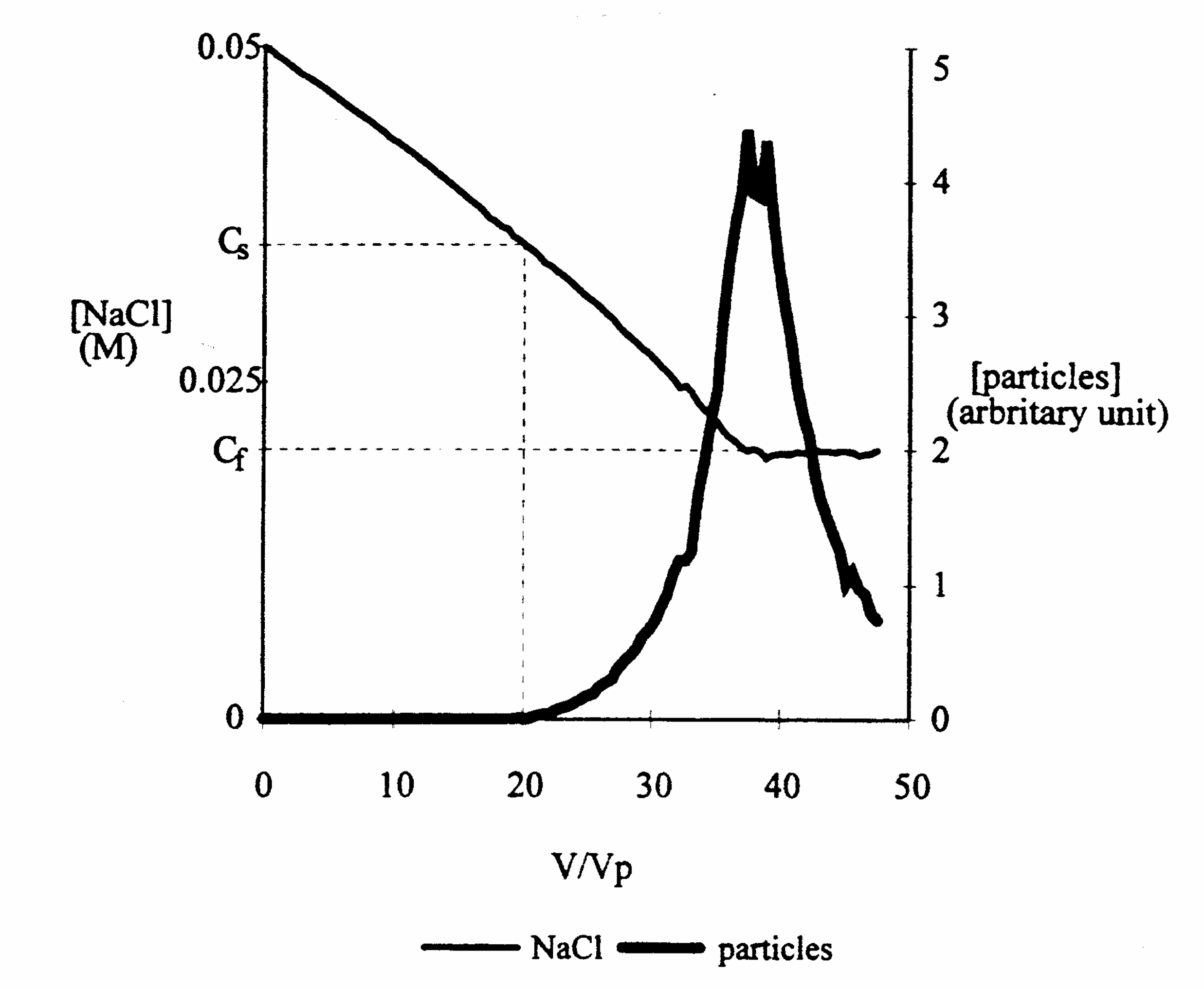

Figure 3. A gradient decrease in ionic strength causes the mobilization of montmorillonite colloids from a quartz sand (95%)/montmorillonite (5%) porous medium [80]. Colloid release begins at $C_s = 0.035$ mol L^{-1} sodium chloride. The supply of mobilized colloids is exhausted in just a few pore volumes (V/V_p; the total volume V divided by a pore volume V_p) at the final sodium chloride concentration, $C_f = 0.019$ mol L^{-1}. The colloid concentration was measured in the column effluent by absorption of ultraviolet light (280 nm wavelength).

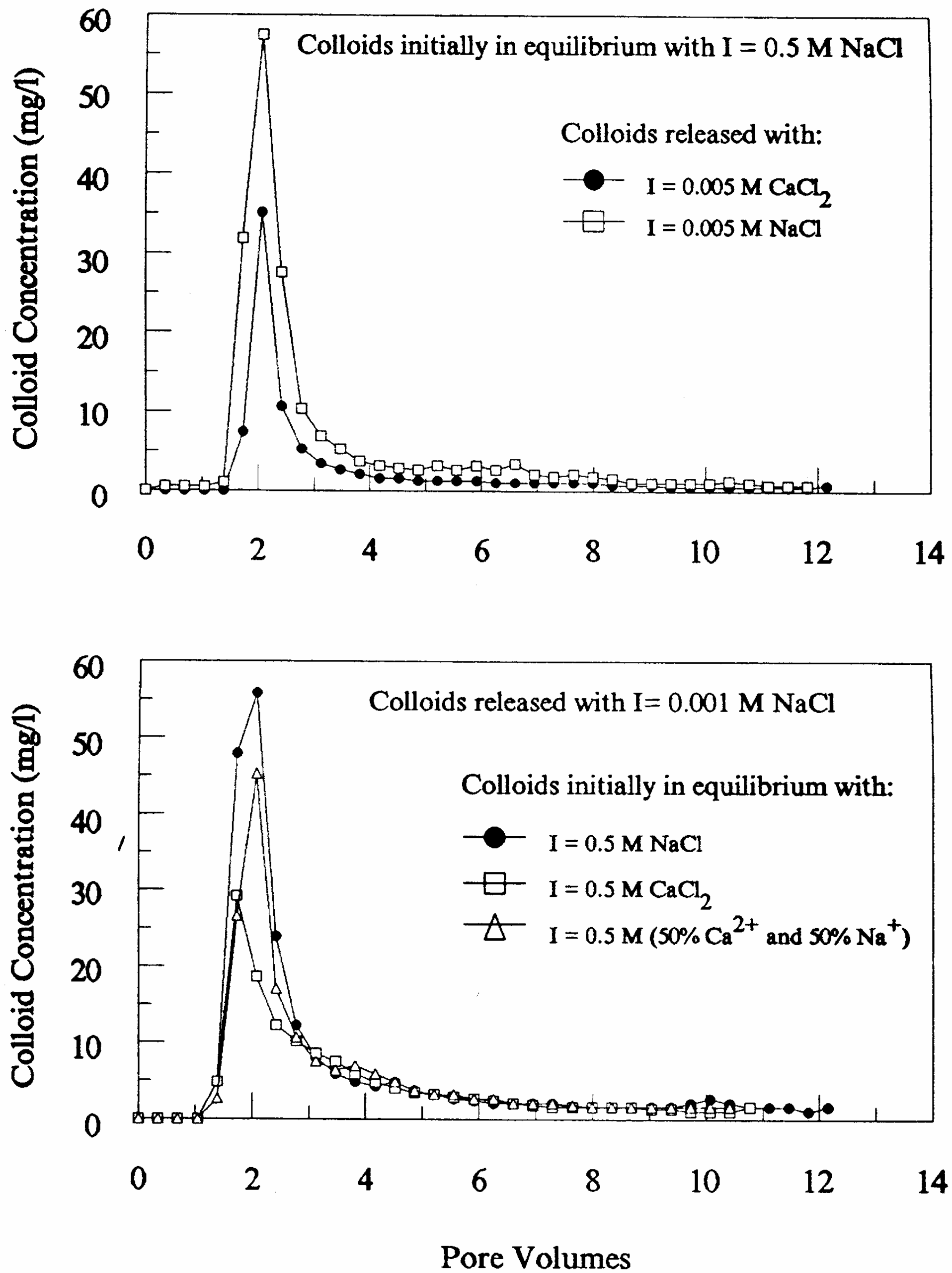

Figure 4. The effect of solution composition on the mobilization of colloids in porous media [83]. In the upper graph, polystyrene latex microspheres deposited on glass in a 0.5 mol L^{-1} NaCl solution are mobilized to a greater extent by lower ionic strength solutions of NaCl than by $CaCl_2$. In the lower graph, the amount of microspheres mobilized decreases as the calcium concentration of the deposition solution increases.

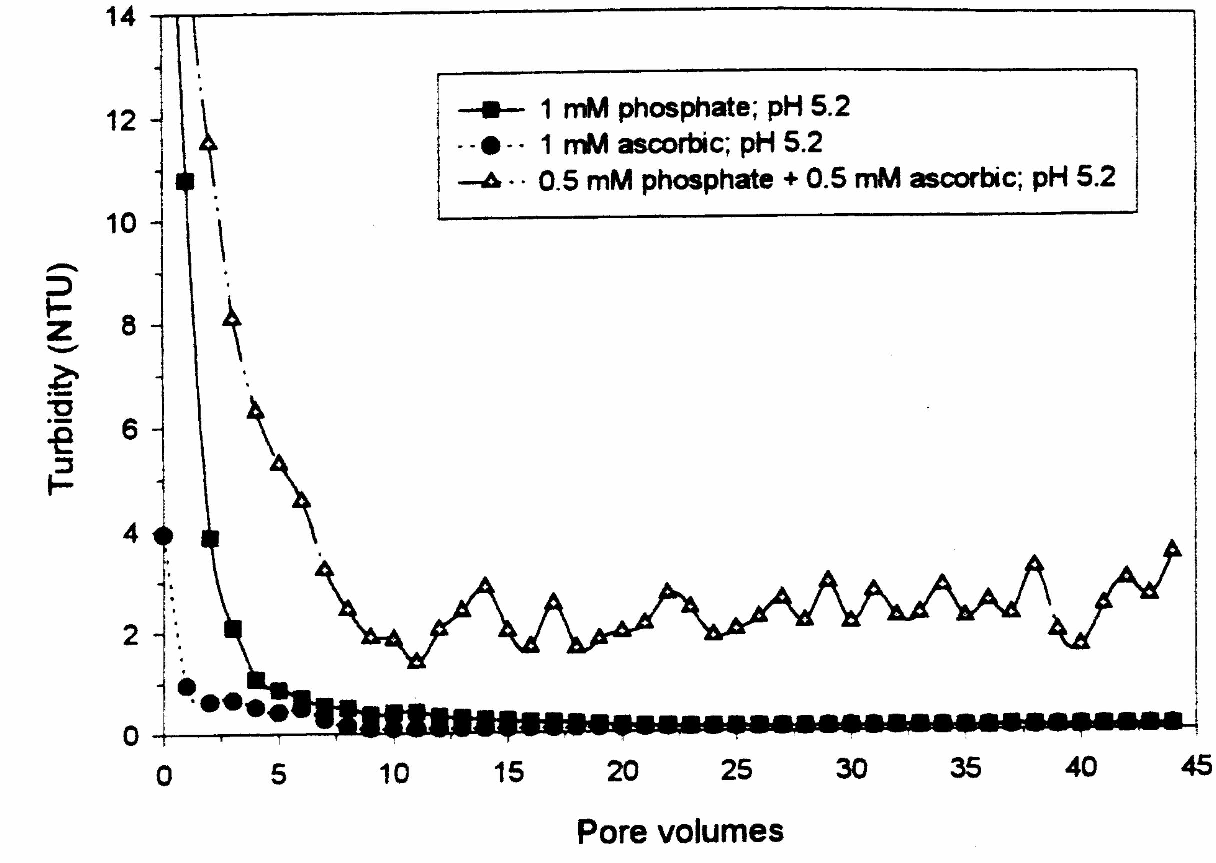

Figure 5. The combination of phosphate and ascorbic acid is much more effective at mobilizing colloids than either the phosphate or ascorbic acid alone [95]. The colloids were mobilized from a southern Atlantic Coastal Plain sediment consisting mainly of ferric oxyhydroxide- and silica-coated quartz grains. Reduction by the ascorbic acid dissolved the ferric oxyhydroxides and adsorption of the phosphate imparted negative charge to the colloids; both of these mechanisms were necessary to mobilize the colloids. The colloid concentration is measured by turbidity as nephelometric turbidity units (NTU).

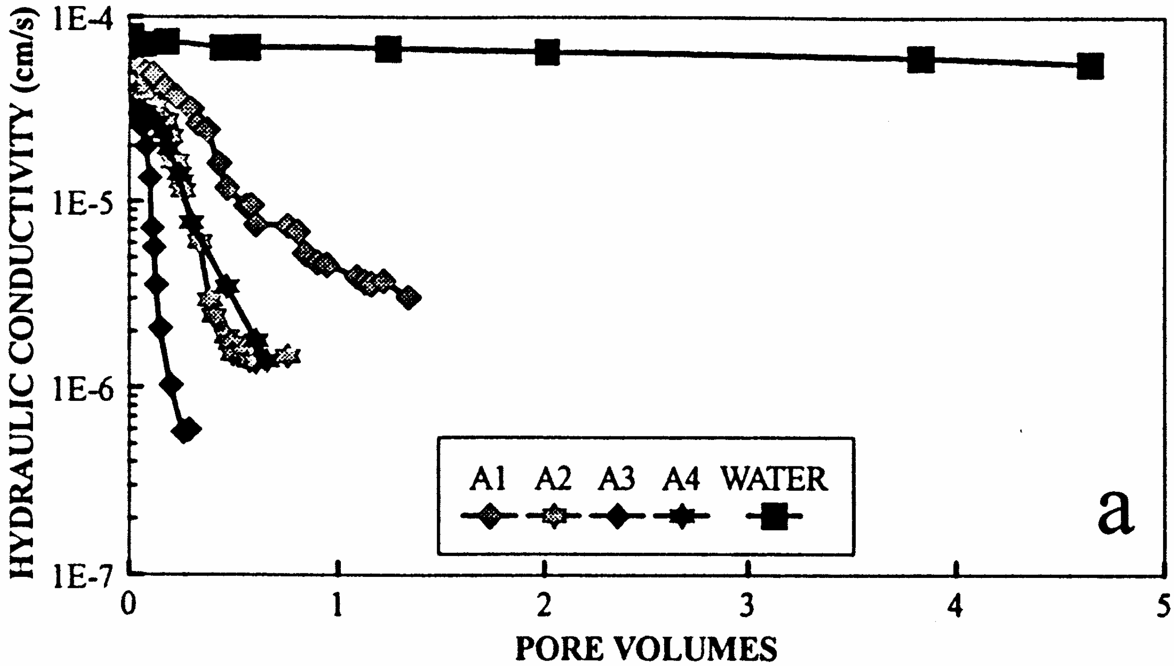

Figure 6. Decreases in the hydraulic conductivity of a loam soil (17% clay) caused by flushing with 0.01 mol kg^{-1} of anionic surfactants A1 (sodium dodecyl sulfate), A2 (sodium alpha olefin sulfonate), A3 (sodium dodecylbenzene sulfonate), and A4 (sodium laureth sulfate) [100].

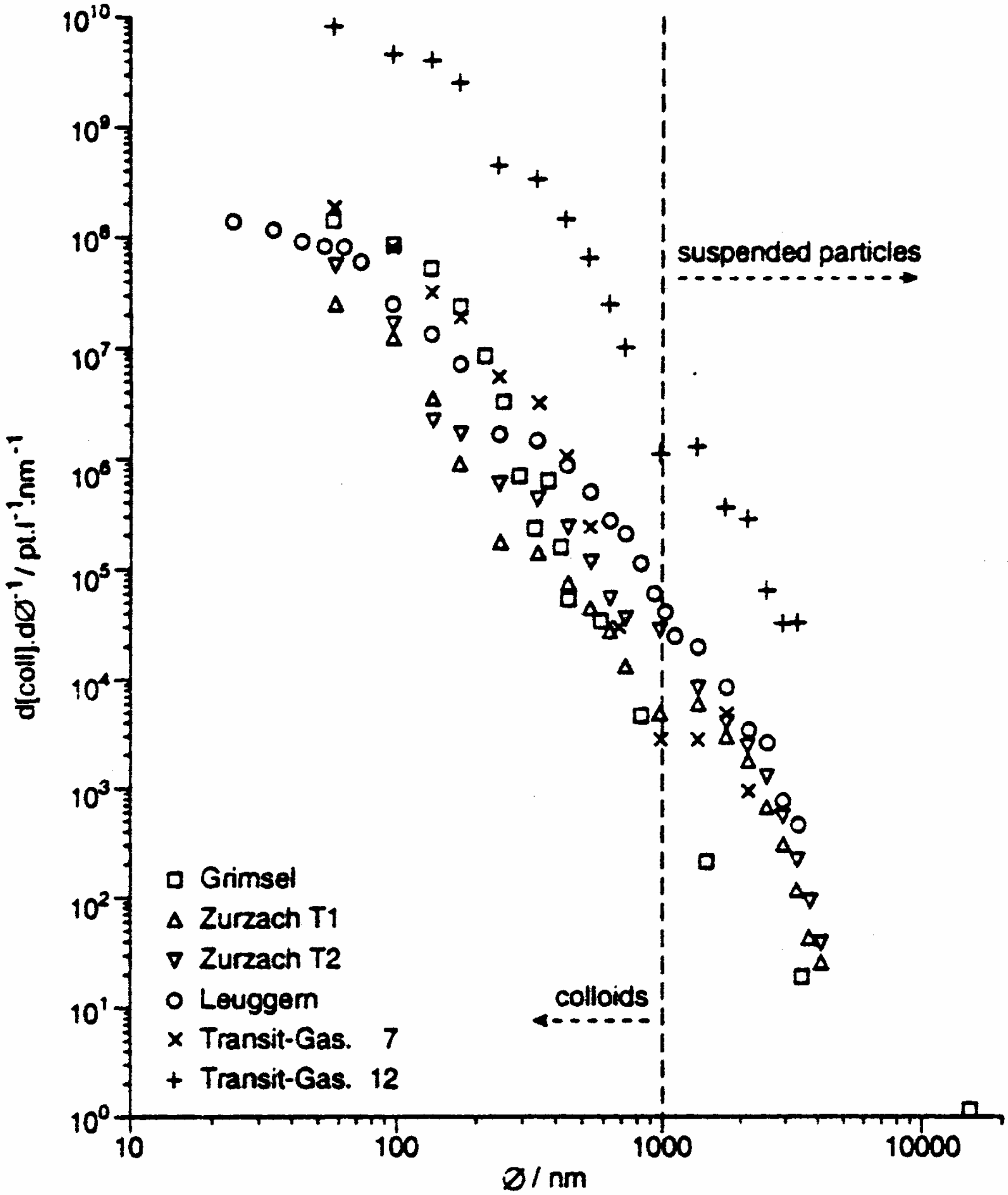

Figure 7. The distribution of colloid size in groundwater samples from fractured granite formations in Europe [113] showing Pareto power law distributions ($N = \mathrm{a}d_p^{-ß}$, where N is the number of colloids in a size range, d_p is the median colloid size in the range, and a and ß are fitting parameters characteristic of the colloid size distribution). These colloid size distributions were measured by single particle counting with scanning electron miscroscopy. The number of colloids per size range is displayed on the *y*-axis and the median size of the range is displayed on the *x*-axis.

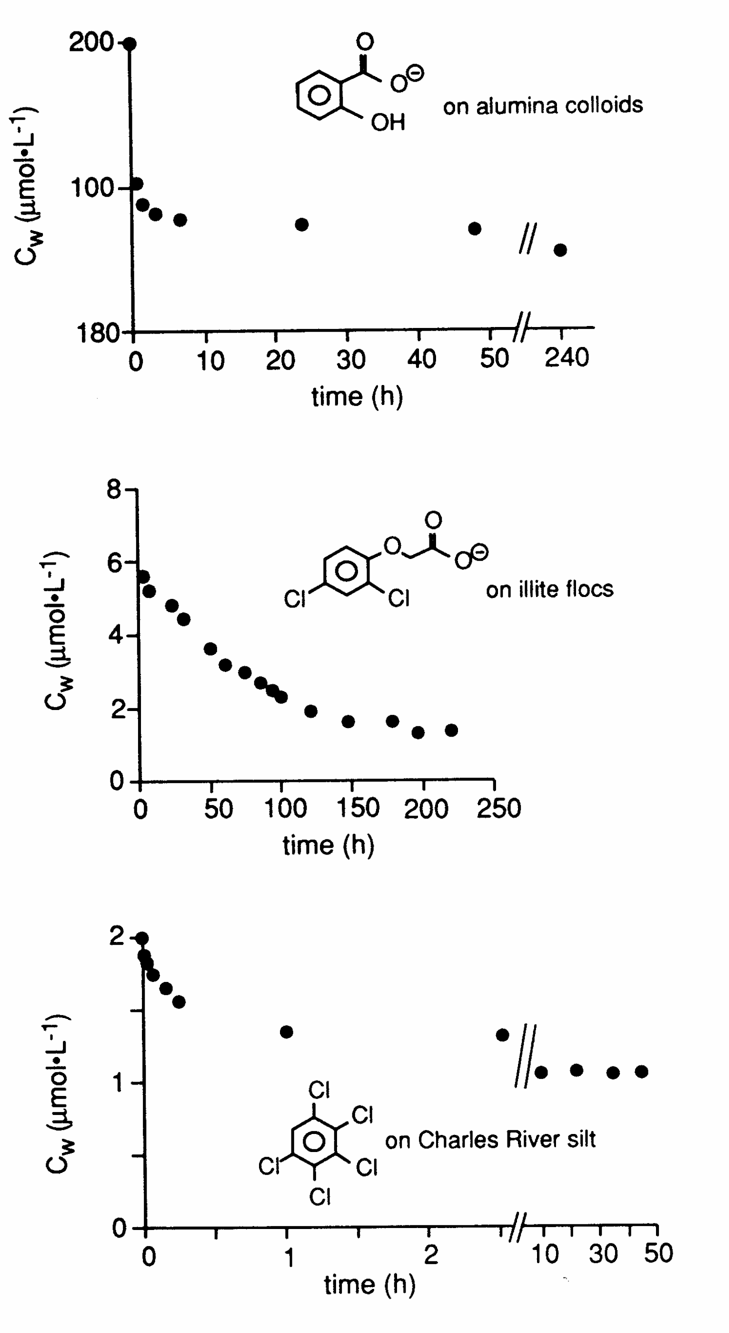

Figure 8. A comparison of the kinetics of contaminant desorption from suspended solids [124]. The vertical axes are the concentration of the compounds in water (C_w). The upper graph shows the desorption of salicylate from 20 nm aluminum oxide colloids. The center graph shows the desorption of (2,4-dichlorophenoxy)acetic acid from clay aggregates. The lower graph shows the desorption of pentachlorobenzene from silt-sized river sediment. The desorption half-life increases as the strength of the contaminant-colloid interaction increases, but the irreversibly sorbed residual varies from case to case.

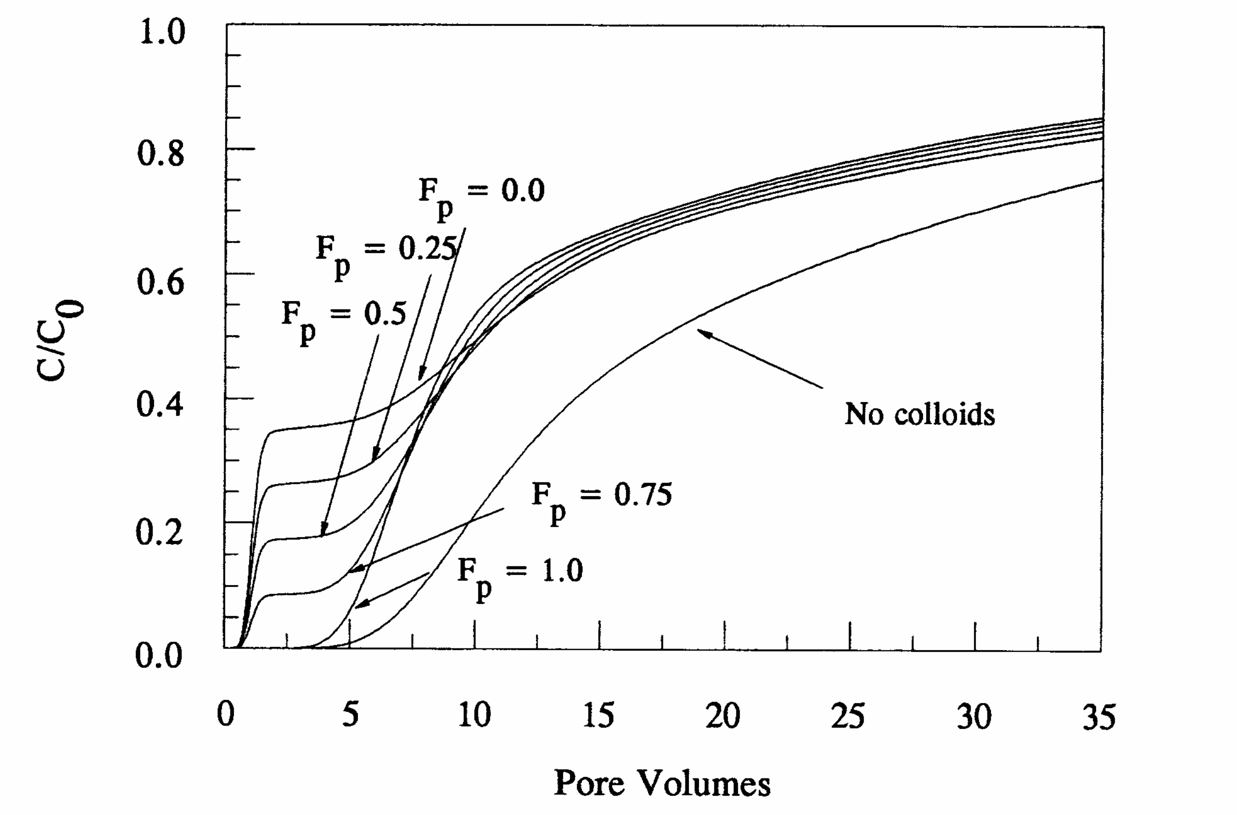

Figure 9. A model simulation of phenanthrene breakthrough as a function of the fraction of reversible sorption sites on colloids (F_p) showing that phenanthrene breakthrough is more rapid when phenanthrene sorption to the colloids is irreversible (F_p = 0) [43]. Sorption was set to be irreversible (the rate of phenanthrene exchange was set to 0 h^{-1}) at the sites not set as reversible. The phenanthrene inlet concentration was C_0 = 1 mg L^{-1}. The colloid concentration was 100 mg L^{-1}. The equilibrium partition coefficient for the phenanthrene association with the colloids was 6,600 mL g^{-1}. The rates of colloid deposition and release were 0.1 and 0.3 h^{-1}.

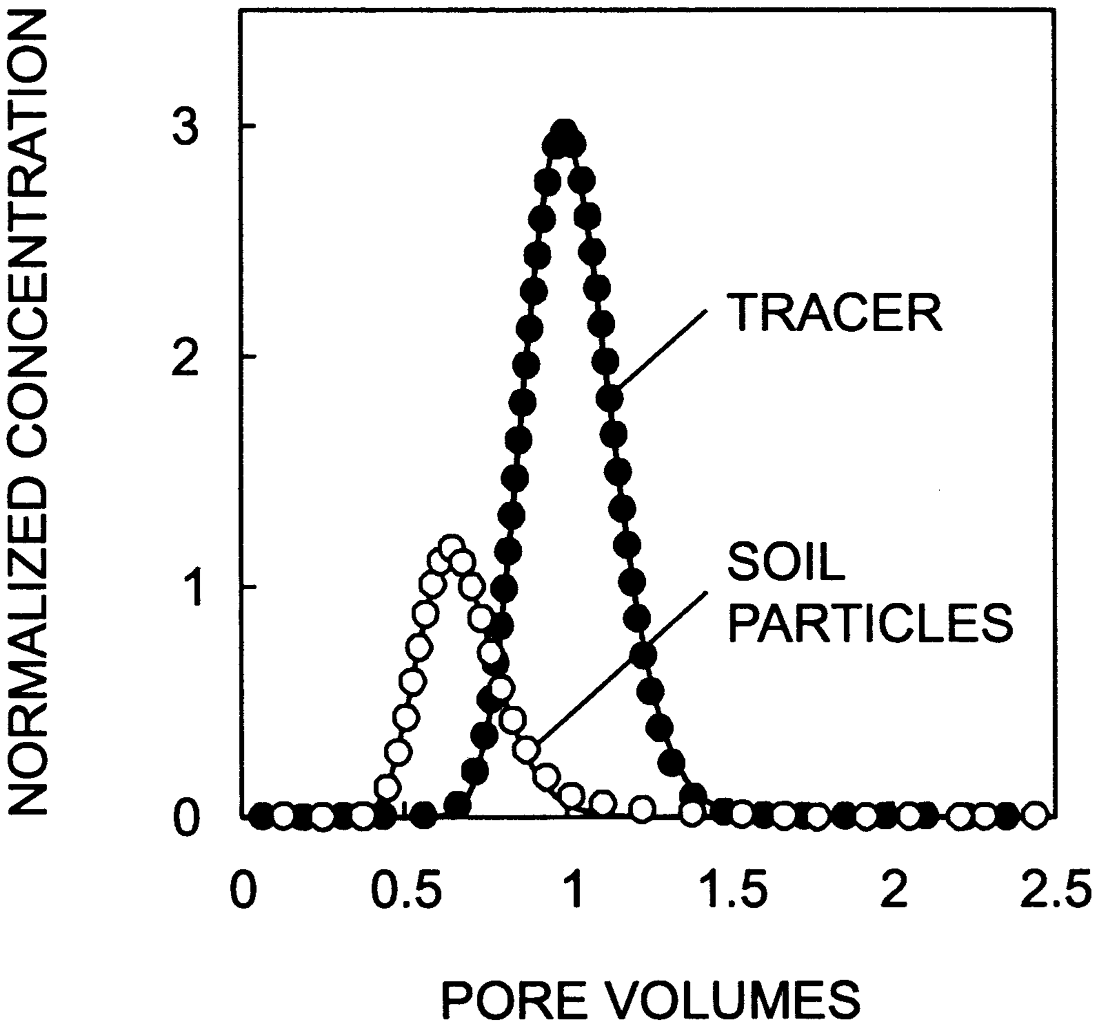

Figure 10. Transport behavior of natural colloidal particles (○) compared to a non-reactive tracer (●) in packed soil columns as a response to a pulse input. The results demonstrate the enhanced transport of the colloidal particles in the heterogeneous soil column due to the phenomenon of size exclusion [154].

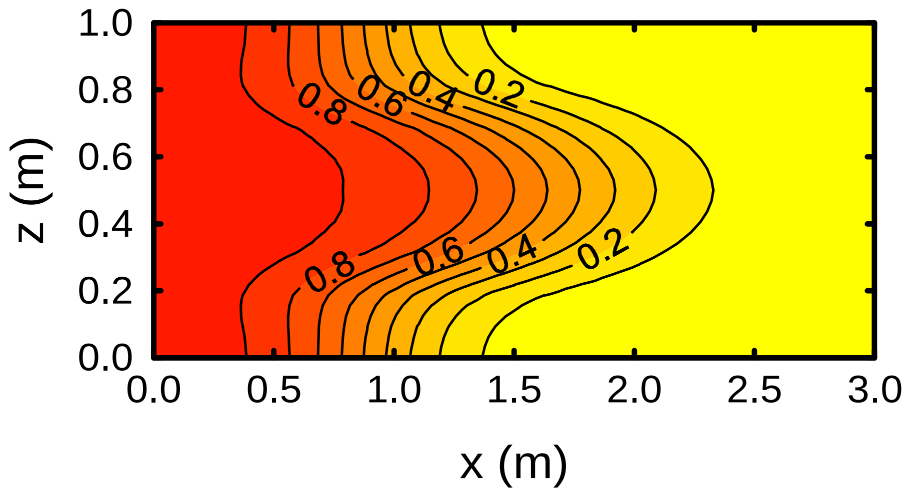

Figure 11**.** Effect of layered physical heterogeneity of porous media on colloid transport behavior. The contours describe the residual particle concentration (C/C_0) at an observation time of 0.75 d. The central layer (*z* between 0.3 and 0.7 m) has hydraulic conductivity *K*=100 m/d and the layers above (*z* between 0.7 and 1.0 m) and below (*z* between 0 and 0.3 m) are with *K*=50 m/d. Colloids are continuously injected along the depth (*z* axis) on the left boundary of the porous medium (*x*=0) [Modified from 163].

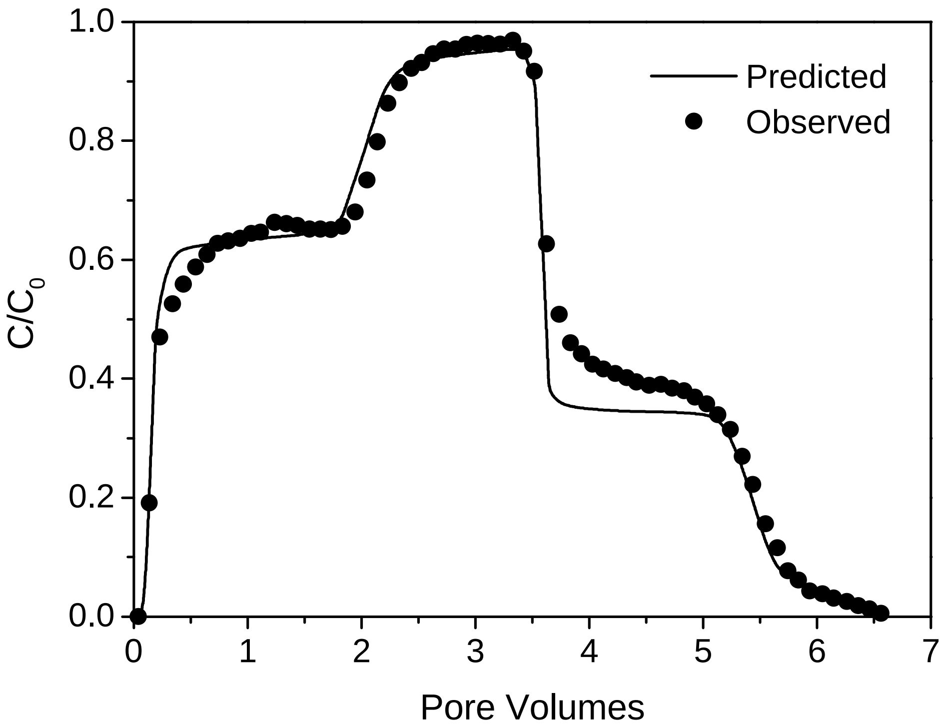

Figure 12. Model prediction and experimental breakthrough curve of colloidal silica particles through a structurally heterogeneous sand column with a distinct preferential flow path [153]. The vertical axis is the normalized concentration (*C*, the concentration in a given pore volume, divided by C_0, the influent concentration).

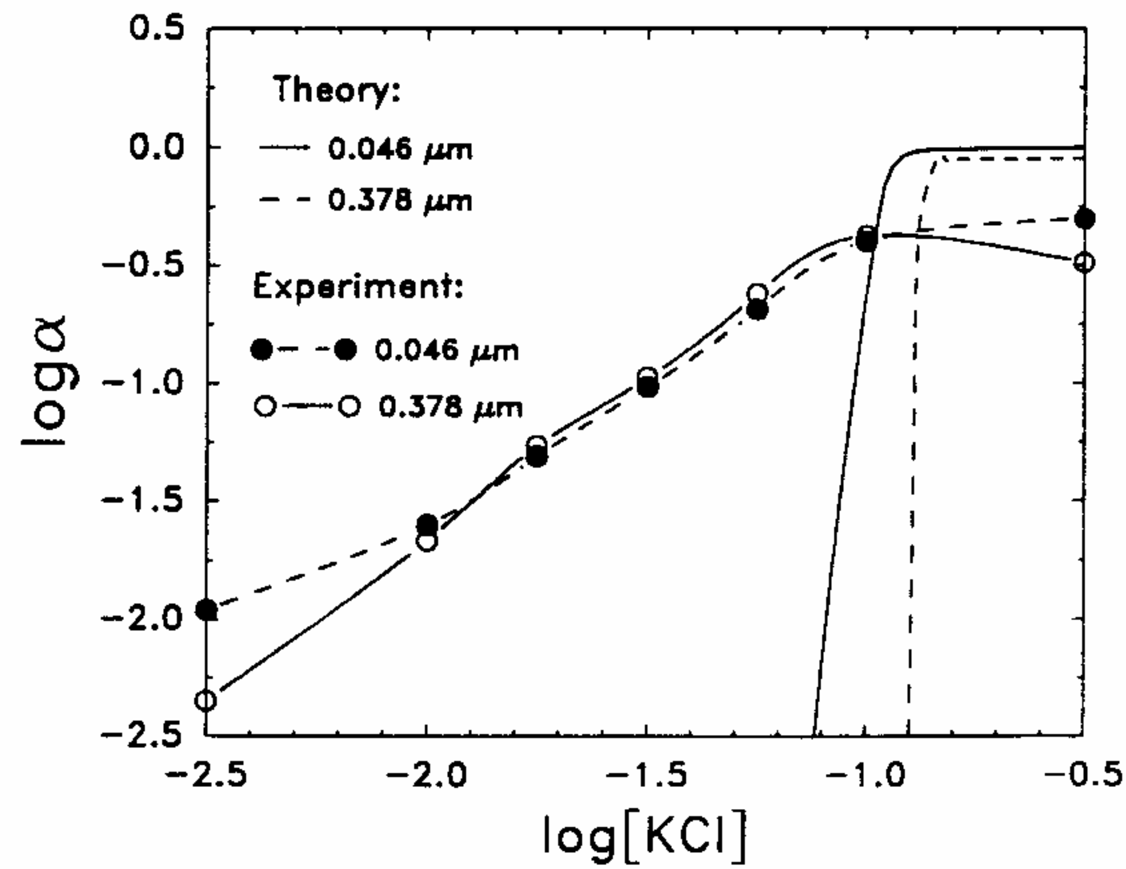

Figure 13. Experimental collision efficiencies (α) of two different suspensions of Brownian polystyrene latex colloids in flow through a column packed with uniform glass beads as a function of KCl concentration. The diameters of the particles are indicated in the figure. Theoretical collision efficiencies shown as lines without data points [Modified from 166].

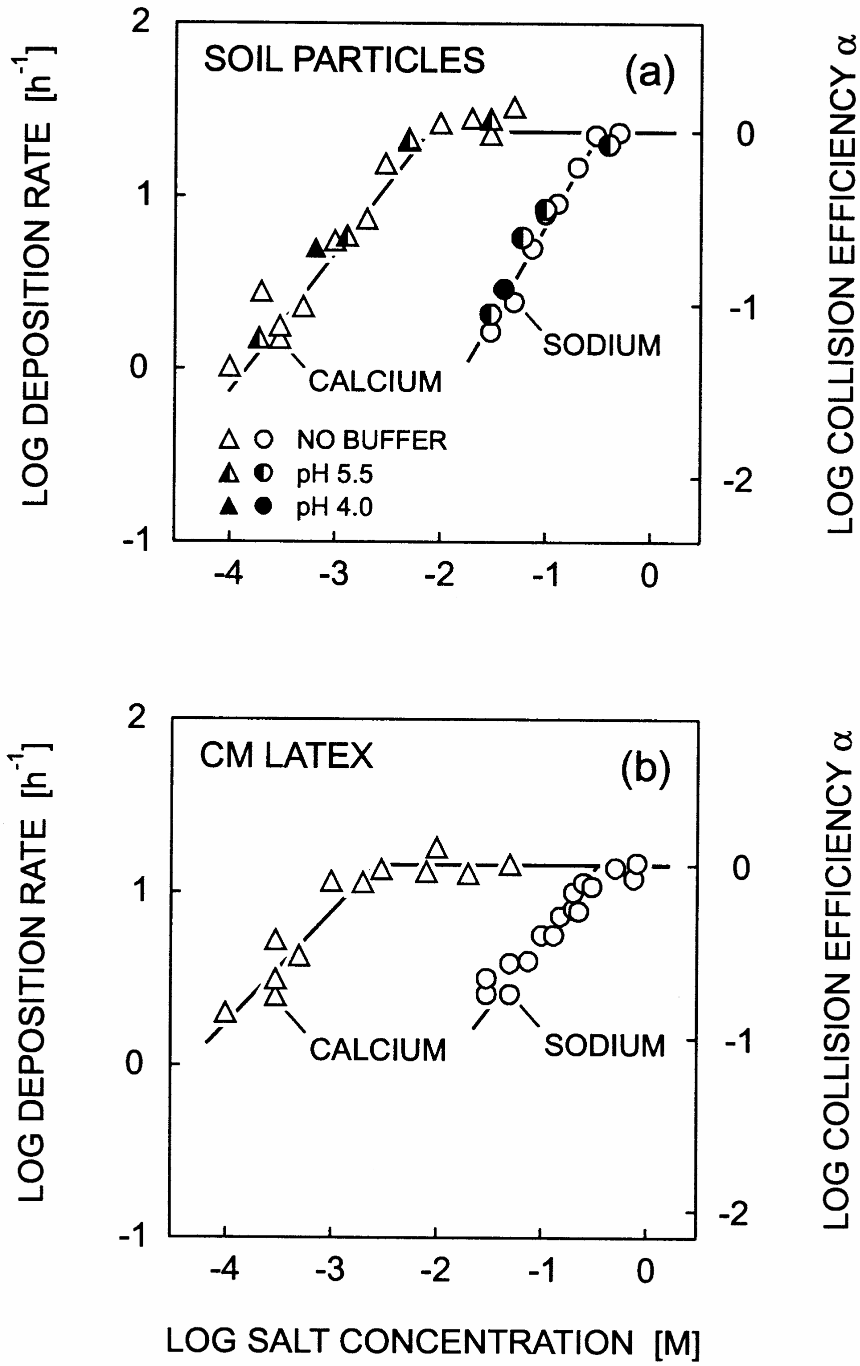

Figure 14. Influence of solution chemistry on particle deposition kinetics in natural porous media (natural soil columns). (a) Effect of electrolyte (NaCl or $CaCl_2$) concentration, counter ion valence (Na^+ and Ca^{2+}), and solution pH (pH 4.0 or 5.5, controlled by azide buffer) on deposition rate coefficients and experimental collision efficiencies for *in-situ* mobilized soil particles. (b) Influence of electrolyte concentration and counterion valence on deposition rate coefficients and experimental collision efficiencies for model carboxyl latex particles. In both figures, solid lines serve to guide the eye [154].

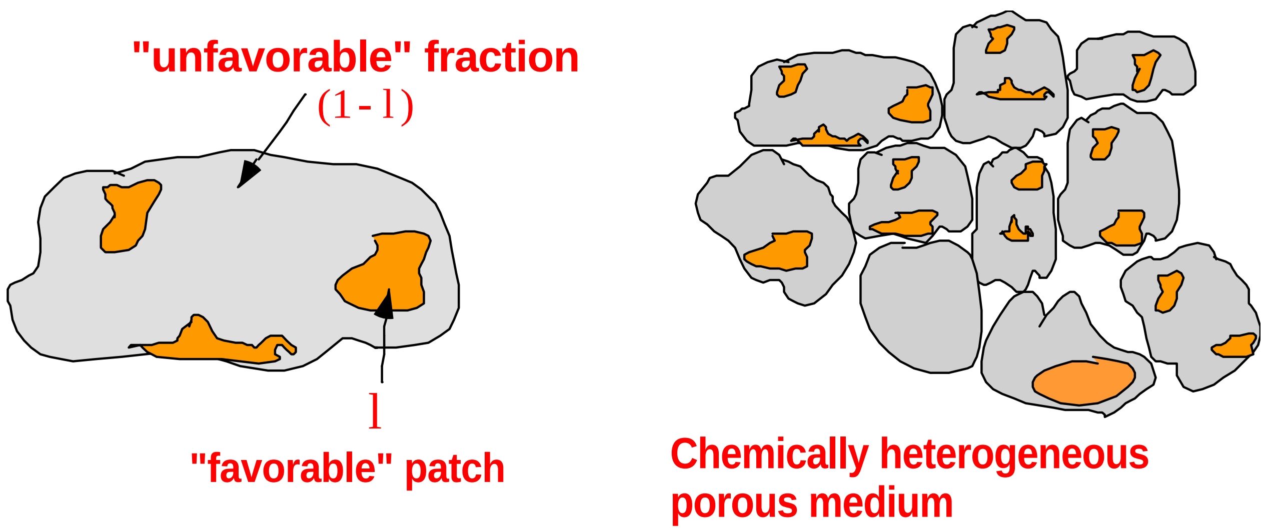

Figure 15**.** Schematic description of the two-patch model for patchwise geochemical heterogeneity. An isolated heterogeneous grain is shown on the left. A representative elementary volume of a geochemically heterogeneous porous medium is shown on the left.

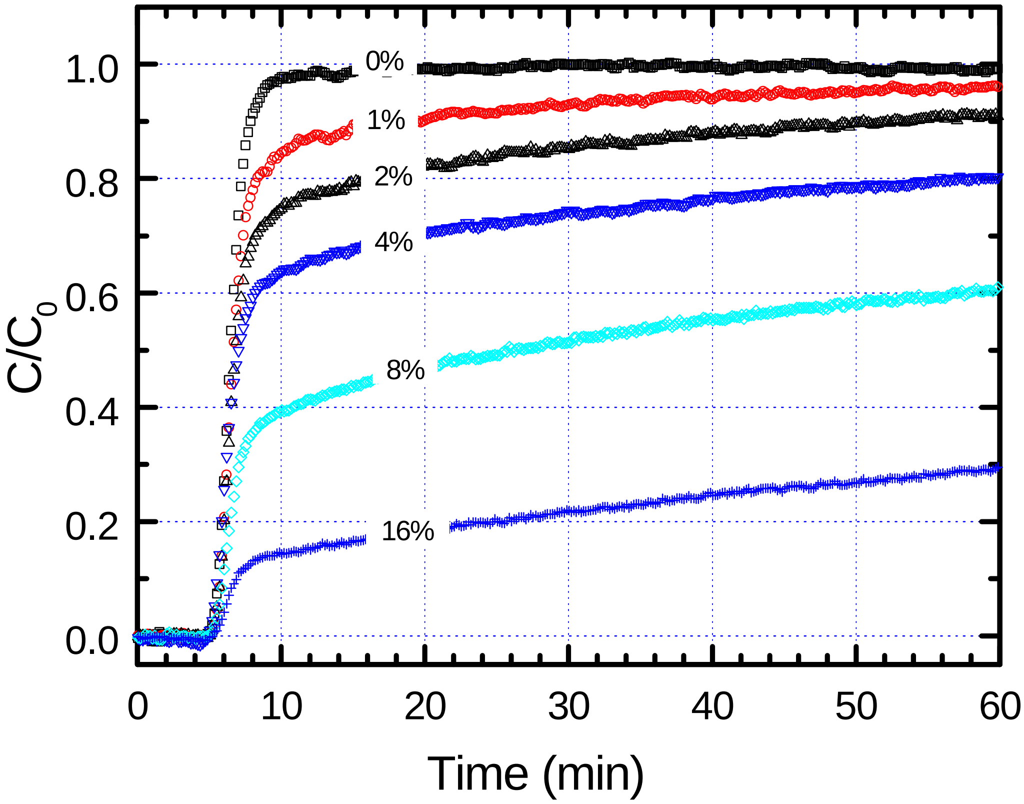

Figure 16**.** Silica particle transport in geochemically heterogeneous porous media. Experimental particle breakthrough curves correspond to columns packed with various fractions of iron oxyhydroxide-coated sand shown in the figure. The vertical axis is the normalized concentration (C, the concentration at a given time, divided by C_0, the influent concentration) [Modified from 173].